Cell Reports
Methods

Article

Methods for culturing adult CNS neurons reveal a CNS conditioning effect

Graphical abstract

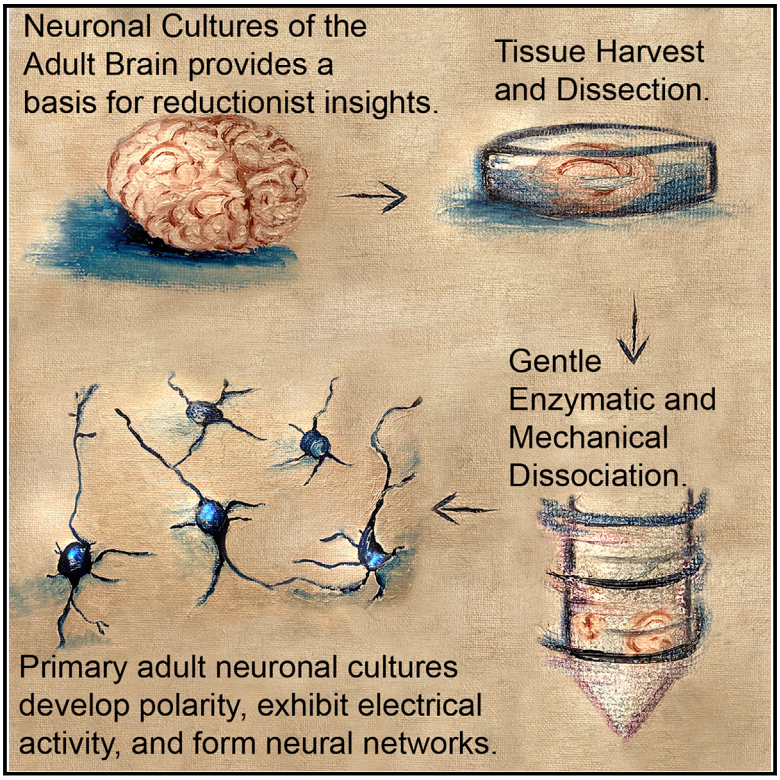

Highlights

- Cultured adult neurons develop polarity with dendrite and axonal compartments
- They exhibit spontaneous and evoked electrical activity *in vitro*
- Cultured adult neurons retain the ability to establish neural networks
- We identify a CNS conditioning effect after spinal cord injury

Authors

Erna A. van Niekerk, Riki Kawaguchi, Camila Marques de Freria, ..., Daniel H. Geschwind, Fred H. Gage, Mark H. Tuszynski

Correspondence

evanniekerk@health.ucsd.edu (E.A.v.N.), mtuszynski@ucsd.edu (M.H.T.)

In brief

van Niekerk et al. report methods for culturing *adult* central nervous system neurons in large numbers and across multiple brain regions for extended time periods. Using adult motor cortex cultures, they identify a CNS "conditioning" effect after spinal cord injury. The ability to culture adult neurons offers a valuable tool for studying basic and therapeutic science of the brain.

van Niekerk et al., 2022, Cell Reports Methods *2*, 100255
July 18, 2022
https://doi.org/10.1016/j.crmeth.2022.100255

CellPress

Cell Reports Methods

CellPress
OPEN ACCESS

Article

Methods for culturing adult CNS neurons reveal a CNS conditioning effect

Erna A. van Niekerk,[1,7,*] Riki Kawaguchi,[2] Camila Marques de Freria,[1] Kimberly Groeniger,[1] Maria C. Marchetto,[3] Sebastian Dupraz,[4] Frank Bradke,[4] Daniel H. Geschwind,[2] Fred H. Gage,[5] and Mark H. Tuszynski[1,6,*]

[1]Department of Neurosciences, University of California, San Diego, La Jolla, CA, USA
[2]Departments of Neurology and Human Genetics, David Geffen School of Medicine, University of California, Los Angeles, Los Angeles, CA, USA
[3]Department of Anthropology, University of California, San Diego, La Jolla, CA, USA
[4]Laboratory of Axon Growth and Regeneration, German Center for Neurodegenerative Diseases (DZNE), Bonn, Germany
[5]Laboratory of Genetics, The Salk Institute for Biological Studies, La Jolla, CA, USA
[6]Veterans Administration Medical Center, San Diego, CA, USA
[7]Lead contact
*Correspondence: evanniekerk@health.ucsd.edu (E.A.v.N.), mtuszynski@ucsd.edu (M.H.T.)
https://doi.org/10.1016/j.crmeth.2022.100255

MOTIVATION *In vitro* model systems have greatly advanced the understanding of neurobiology. To date, these model systems have consisted of either embryonic or early postnatal brain cultures or cultures of adult dorsal root ganglion neurons. It has not been widely possible, however, to culture adult brain neurons. We report methods that enable culturing neurons from the adult mouse brain taken as late as 60 days postnatally. Neurons can be cultured in large numbers and maintained *in vitro* over several weeks. Cultured adult neurons can be readily attained from all brain regions sampled and closely resemble neurons phenotypically of their native region.

SUMMARY

Neuronal cultures provide a basis for reductionist insights that rely on molecular and pharmacological manipulation. However, the inability to culture mature *adult* CNS neurons limits our understanding of adult neuronal physiology. Here, we report methods for culturing *adult* central nervous system neurons in large numbers and across multiple brain regions for extended time periods. Primary adult neuronal cultures develop polarity; they establish segregated dendritic and axonal compartments, maintain resting membrane potentials, exhibit spontaneous and evoked electrical activity, and form neural networks. Cultured adult neurons isolated from different brain regions such as the hippocampus, cortex, brainstem, and cerebellum exhibit distinct cell morphologies, growth patterns, and spontaneous firing characteristics reflective of their regions of origin. Using adult motor cortex cultures, we identify a CNS "conditioning" effect after spinal cord injury. The ability to culture adult neurons offers a valuable tool for studying basic and therapeutic science of the brain.

INTRODUCTION

In 1910, Harrison published the first report of frog embryonic sympathetic ganglia grown in hanging drops of lymph for several days, where single neurons extended neurites with complex growth cones, protruding and retracting over time toward target cells (Harrison, 1910). Subsequently, neuronal culture methods were developed that were consistently successful in sustaining developing and early postnatal central nervous system (CNS) neurons *in vitro* (Carrel, 1923; Scott, 1977). Techniques for culturing neural progenitor cells from the adult subventricular zone and hippocampus were described in the early 1990s (Reynolds and Weiss, 1992; Suhonen et al., 1996; Lois and Alvarez-Buylla, 1994; Levison and Goldman, 1993). Yet cultures of mature adult neurons have not to date been consistently achieved. The inability to culture adult CNS neurons stands in contrast to techniques for successfully culturing adult dorsal root ganglia (DRG) neurons (Smith and Skene, 1997; Ylera et al., 2009), which have yielded critical insights into understanding of neuronal genetics, physiology, and function.

Developing methods to culture mature adult CNS neurons may be key to advancing our understanding of neuronal function and neuronal responses to injury and degeneration. Moreover, adult neuronal cultures would constitute useful screens for

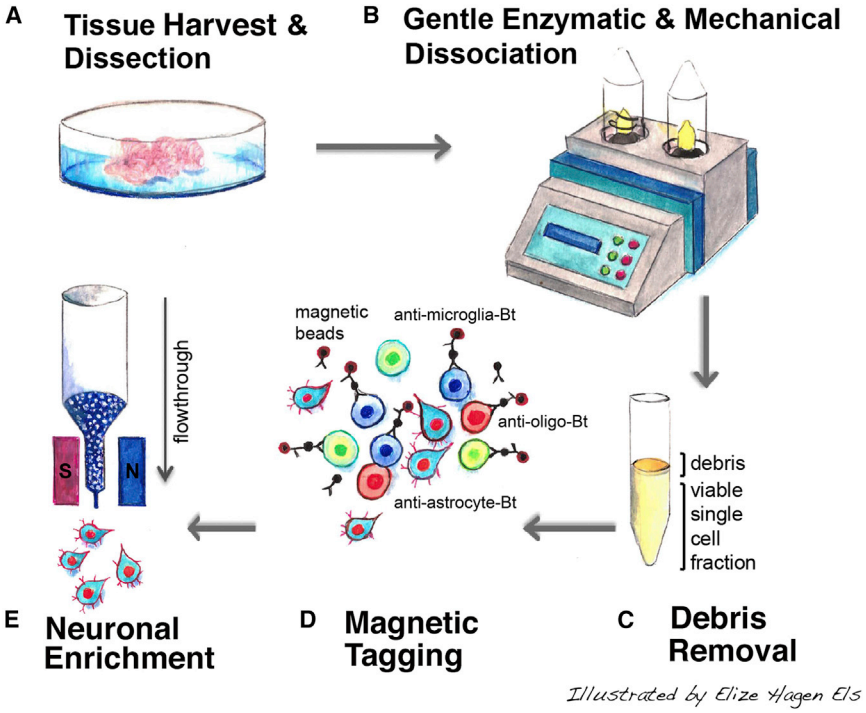

Figure 1. Methods for culturing adult primary CNS neurons

(A) Tissue is harvested rapidly under cold conditions.

(B) Enzymatic-buffer solution containing DNase and papain is used with very gentle mechanical dissociation to slowly disrupt tissue.

(C) Debris mostly consisting of dead cells and myelin is removed.

(D) Magnetic biotinylated antibodies are added against cell surface markers of astrocytes, oligodendrocytes, microglia, and endothelial cells to deplete non-neuronal cells.

(E) A cell-antibody magnetically labeled mixture is loaded onto a ferromagnetic sphere column and magnetically labeled cells remain in column while non-magnetically labeled cells (primarily neurons) are eluted from column, resulting in neuronal enrichment.

candidate therapeutics. Here we report for the first time the development of a method to consistently culture mature adult neurons in large numbers over extended time periods, including hippocampal, cortical, brainstem, and cerebellar neurons. Cultured adult neurons retain many characteristics of their *in vivo* regional brain identity. We also provide evidence for the utility of these cultures in advancing studies of CNS injury, demonstrating a "central conditioning" effect after spinal cord injury on cortical motor neurons and on the transcriptome associated with this state that mirrors several features of the injured *in vivo* transcriptome (Chandran et al., 2016).

RESULTS

Methods to successfully culture mature adult CNS neurons were based on modifications to protocols by Miltenyi Biotec (https://www.miltenyibiotec.com/upload/assets/IM0011920.PDF). Using the original protocol provided by the company, we were unable to successfully culture mature CNS neurons, but with modifications, the procedure consistently yielded cultures of tens of thousands of neurons per brain region. A key feature of the method is utilization of extremely gentle mechanical and enzymatic dissociation of CNS tissue. Applied up to postnatal day (PND) 90 cortical regions, the longest time point tested, neurons and their processes were gently teased apart from their intricately interwoven projections to other neurons and the neuropil, allowing successful culture of large numbers of adult neurons.

To start, individual regions of the adult mouse brain, including motor cortex, hippocampus, striatum, cerebellum, or brainstem, were grossly dissected as single 4- to 8-mm blocks. This step was a departure from the company's instructions, which were to use whole brain. We were unable to successfully culture mature adult neurons when starting with whole brain. Individual brain regions were therefore removed as single, separate blocks of tissue and processed separately without further dissection. Instructions from the manufacturer recommended "chopping" brain tissue after dissection into smaller blocks, but this resulted in unsuccessful cultures in our hands. Thus, tissue blocks from each brain region were left intact to minimize trauma.

Blocks were then immersed in Dulbecco's PBS containing glucose, calcium, magnesium, sodium pyruvate, and antibiotics (see STAR Methods for concentrations and details). After 1 to 2 min in this solution, the tissue blocks were removed, rinsed, and immersed in a solution containing the enzymes papain and DNAse and placed into a very gentle mechanical dissociator (Octo Dissociator; Miltenyi.) at 37°C for 30 min (Figure 1; Table 1). The dissociator gently agitated tissue without exerting excessive shear force, thereby contributing to a gradual dissociation and separation of neural components. The resulting tissue was then subjected to a more harsh step of passing through a 70-μm filter, and then washed and centrifuged at 300 × *g* at 4°C for 10 min.

Supernatant was discarded and cells were resuspended in a Percoll solution followed by the addition of an equal overlying volume of Dulbecco's solution, creating two phases. This density gradient was centrifuged at 3,000 × *g* at 4°C for 10 min, resulting in cells, including neurons, glia, endothelial cells, and red blood cells, occupying the bottom phase and debris in the interphase. The top and interphase were gently removed and discarded, and cells in the bottom phase were washed and centrifuged at 1,000 × *g* at 4°C for 10 min. The supernatant was discarded. The next step of the original protocol lysed red blood cells using a solution of ammonium chloride, a permeabilizing electrolyte for red blood cells. However, this protocol was excessively harsh on neurons in our hands and prevented successful completion of the protocol to obtain surviving neurons. Thus, we added 20 ng/mL of brain derived neurotrophic factor (BDNF) to the

Table 1. Reagents and equipment

1. Tissue culture incubator at 37°C with 5% CO_2
2. Tissue culture hood
3. GentleMACS Octo Dissociator with Heaters (Miltenyi, 130-096-427)
4. Centrifuge with a swinging bucket rotor that can achieve 3,000 × *g* at 4°C
5. MidiMACS separator (Miltenyi, 130-042-302)
6. Adult brain dissociation kit (Miltenyi, 130-107-677)
7. Adult neuron isolation kit (Miltenyi, 130-125-603)
8. Dulbecco's PBS (DPBS), calcium, magnesium, glucose, pyruvate (Gibco, 14287072)
9. DPBS, calcium, magnesium (Gibco, 14040141)
10. C-tubes (Miltenyi, 130-096-334)
11. LS-columns (Miltenyi, 130-042-401)
12. 10% BSA sterile stock solution (Miltenyi, 130-91-376)
13. 6-well plate (Sigma, CLS3506-100EA)
14. Brain derived neurotrophic factor (Peprotech, 450-02)
15. MACS neuro media (Miltenyi, 130-093-570)
16. B27 (Gibco, 17504044)
17. 100X Glutamax (Gibco, 35050061)
18. 100X Pen/strep (Sigma, P4333-20ML)
19. Fetal bovine serum (Gibco, 26140)
20. 15-mL and 50-mL conical tubes
21. 70-μM cell strainer (Falcon, 352350)
22. 0.01% poly-L-lysine (Sigma, P4707-50ML)
23. Laminin (Sigma, L2020)
24. Double distilled H_2O (Invitrogen, 10-977-023)
25. Culture vessel (i.e., Nunc Lab-Tek II 8-well chambered slide, Sigma, Z734853-96EA)

cell solution at this stage, since BDNF acts as a survival factor for mature cortical neurons (Giehl and Tetzlaff, 1996; Nagahara et al., 2009). With this modification, the protocol was successful. After this step, the cell mixture was reconstituted in BSA and Dulbecco's solution and centrifuged again at 300 × *g* at 4°C for 10 min.

Next, neurons were enriched using a negative selection process by adding a cocktail of biotinylated antibodies directed against astrocytes (anti-astrocyte-biotin), oligodendrocytes (anti-oligodendrocyte-biotin), microglia (anti-microglia-biotin) and endothelial cells (anti-endothelial-biotin), per company instructions. After a 5-min incubation in this antibody solution at 4°C, cells were washed and centrifuged at 300 × *g* at 4°C for 10 min. Supernatant was discarded and the cell pellet was gently resuspended in streptavidin magnetic beads for 10 min. Next, 400 μL of cell culture media was added containing MACS neuro media supplemented with Glutamax, Pen/strep, B27, and 10% fetal bovine serum. This cell/antibody mix was placed onto an LS magnetic column containing ferromagnetic spheres: non-neuronal cells adhered to magnetic beads while neurons passed through the column and were collected (Figures 2H and S1A). Then, 20 ng/mL of BDNF was added to the eluted cells and neurons were cultured on laminin substrates or astrocyte feeder layers at a concentration 3 to 4 × 10^4 cells/cm^2 in the media described above for up to 2 weeks.

This cell isolation method resulted in viable, mature adult brain cultures that consisted of 82.9% ± 0.4% neurons, 8.6% ± 2.6% astrocytes, 3.4% ± 1.2% oligodendrocytes, 1.2% ± 0.5% microglia, and 2.1% ± 0.8% endothelial cells (Figures 2H, S1A, and S2C–S2E). Cultures were successfully generated from mice ranging from 28 to 90 days (the oldest age attempted) post-natally, and cells survived for at least 14 days (the longest time point tested) in culture. The column purification step eluted 75% of the original number of neurons added to the column in the crude cell mixture (Figure S1B). A single brain region such as the motor cortex consistently yielded a mean of 10,280 ± 940 neurons by fluorescence-activated cell sorting (FACS) analysis (Figure S1D). The proportion of viable cells at the time of elution from the column was 93.6% ± 1.9% by calcein AM positive signal (Figure S1F). The proportion of dead cells at the time of elution from the column was 2.1% ± 0.5% based on propidium iodide exclusion (Figure S1G), and 94.6% ± 1.1% of cells were in single cell suspension (Figure S1E). FACS indicated that 89.7% ± 3.3% of isolated neurons expressed the excitatory neuronal marker VGlut1, and that 7.5% ± 1.8% expressed the inhibitory marker GAD67 (Figures S1H–S1M).

Adult neuronal cultures can be established from multiple brain regions

Adult neurons in culture from various brain regions retained several features characteristic of their *in vivo* cell morphology (Figures 2A and S2F): motor cortex neurons exhibited pyramidal morphology and long single axons (Figures 2E, 3D, and S2F); cerebellar Purkinje neurons were large with complex dendritic-like neurites and expressed calbindin (Figures 2A and S2F); some hippocampal neurons exhibited multiple radial processes; reticulospinal (brainstem) neurons (identified by injections of cholera toxin B into the C7 segment of the ventral spinal cord)

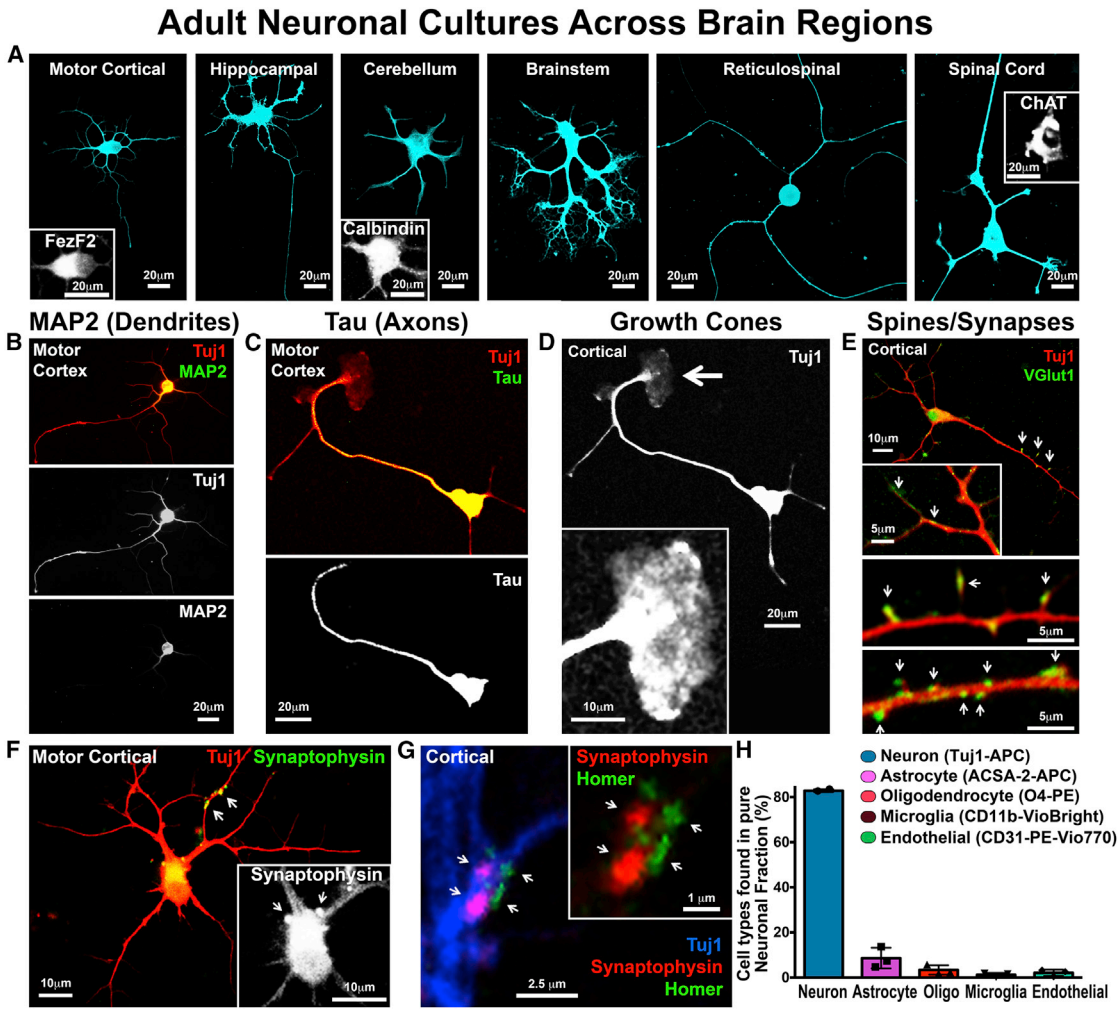

Figure 2. Adult CNS neuron cultures

(A) Neurons from different CNS regions exhibit distinct phenotypic characteristics. Labeling for neuronal marker **Tuj1**. FezF2 (inset) identifies layer 5b glutamatergic neurons. Cerebellar Purkinje cell neuron labels for calbindin (inset) and spinal cord neuron labels for choline acetyltransferase (ChAT, inset). Neurons isolated at age 6 weeks. Scale bars, 20 μm.

(B) Motor cortex neurons form distinct dendritic compartments identified by MAP2 after 5 days *in vitro*. Tuj1 red, MAP2 green. Neurons isolated at age 6 weeks. Scale bar, 20 μm.

(C) Tau labeling (green) identifies axons in culture. At the axon tip is a growth cone. Tuj1 red, with Tau only panel shown below. Neurons isolated at age 4 weeks and cultured for 5 days *in vitro*. Scale bar, 20 μm.

(D) Growth cone (arrow and inset) with lamellipodia is evident in cortical cultures isolated at age 4 weeks, with 7 additional days *in vitro*. Labeled for Tau. Scale bar, 20 μm.

(E) Vesicular glutamate-1 (**VGlut1**) is present in soma and at bouton-like structures (arrows) indicating excitatory synapses. Tuj1 red. Neurons isolated at age 6 weeks. Scale bars, 10 and 5 μm.

(F) Synaptophysin boutons present on motor cortical cell bodies and on Tuj1-labeled neurites. Neurons were isolated at age 6 weeks. Scale bar, 10 μm.

(G) Post-synaptic marker **Homer** (**green**) localizes with the presynaptic marker synaptophysin (**red**) at the junction of two **Tuj1**-labeled processes (**blue**), indicating a synapse (arrows). Inset with **Homer** and **synaptophysin**. Neurons isolated at age 9 weeks. Scale bars, 1 and 2.5 μm.

(H) FACS analysis of enriched neuronal fraction. 82.8% of cells are neuronal, 8.6% astrocytes, 3.37% oligodendrocytes, 1.18% microglia, and 2.08% endothelial cells. Flow cytometry antibodies: neurons (Tuj1), astrocytes (ACSA), oligodendrocytes (O4), microglia (CD45, CD11b), and endothelial cells (CD31). Flow cytometry dyes include APC (allophycocyanin), PE (phycoerythrin), VioBlue, VioBright-FITC, and PE-Vio770. Cells isolated at age 8 weeks. Error bars = STDEV.

exhibited strikingly long processes up to 0.8 mm in length (Figures 2A and 3E); and spinal cord alpha motor neurons were large, exhibited distinct pyramidal morphology and expressed choline acetyltransferase (ChAT; Figures 2A and S2F). Subsets of cortical motor neurons could be identified by injections of retrogradely transported tracers; for example, corticospinal neurons, which possess some of the longest axons of the nervous system and have previously been extraordinarily difficult to culture in adults, exhibited large pyramidal morphology and expressed the characteristic transcription factor Fezf2

CellPress
OPEN ACCESS

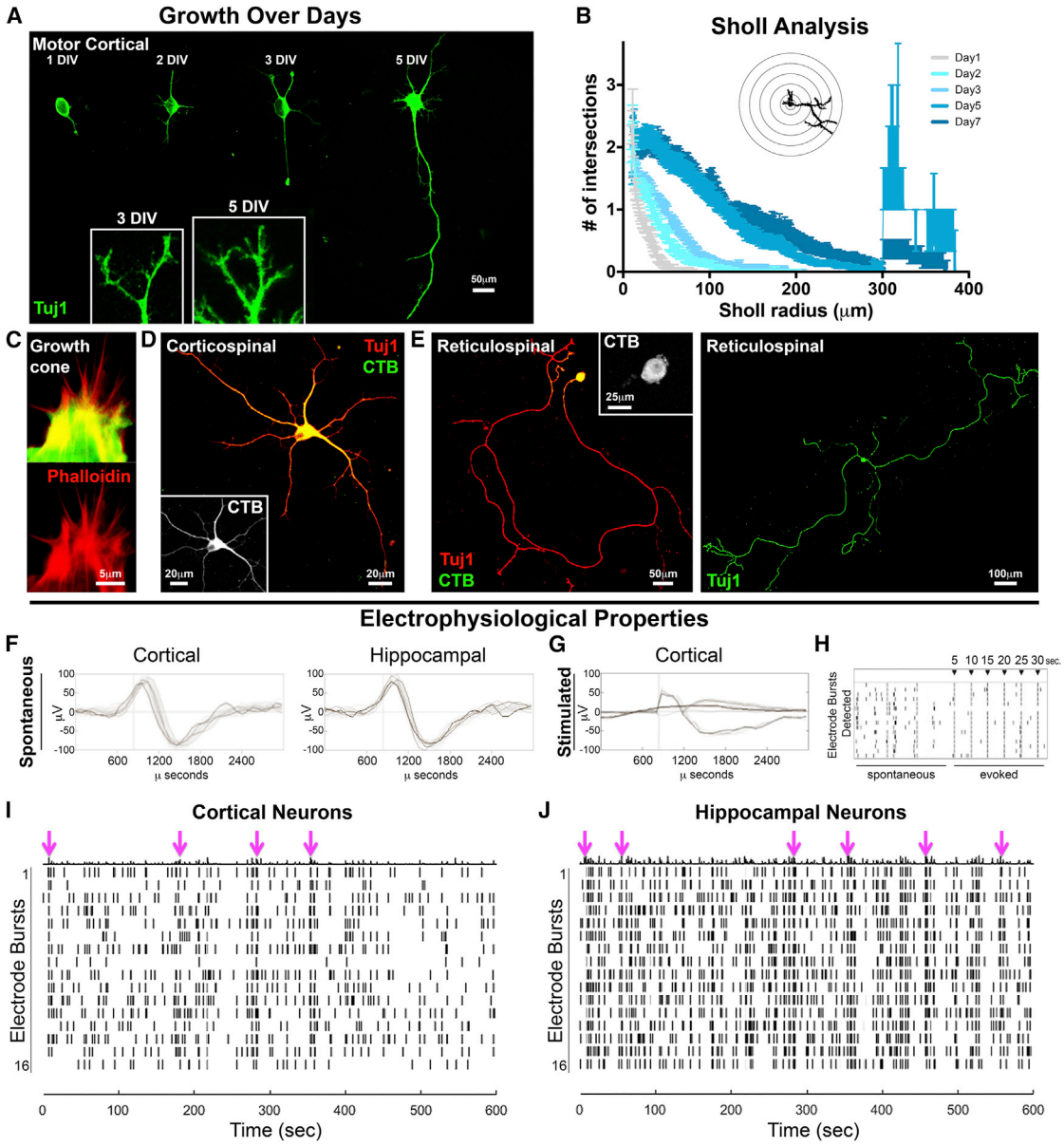

Figure 3. Spontaneous neural growth and electrical activity

(A) Neuritic outgrowth from adult cortical neurons over 5 subsequent days. Dendrites are visible after 3 days (inset). Tuj1 labeling. Scale bar, 50 μm. Neurons isolated from 6-week-old animals. Image is a composite.

(B) Sholl analysis of neuritic "crossings" of Tuj1-labeled processes at 1-μm interval distances from centroid. Data represent 50 neurons measured at every time point in culture from motor cortex ± SEM.

(C) **Phalloidin** labeling (**red**) of cortical growth cone in culture (red) and **Tuj1** (**green**). **Phalloidin** only panel below. Scale bar 5 μm.

(D) Corticospinal neurons identified by CTB retrograde tracer injections into C8 spinal cord. Motor cortex cultures harvested at age 9 weeks and maintained *in vitro* 5 days. Scale bars, 20 μm.

(E) Reticulospinal neurons identified by CTB retrograde tracer injections into C8. Brainstem cultures isolated at 9 weeks. **Tuj1 red, CTB green**. Scale bars, 25, 50, and 100 μm.

(F) Electrophysiological activity in cultured adult cortical and hippocampal neurons. Neurons isolated from 6-week-old mice, plated onto microelectrode arrays and cultured for 10 days *in vitro*. Spontaneous electrical activity is evident.

(G) Evoked activity is present after stimulation at 500 mV for 400 μs every 5 s. Recordings from other cells simultaneously indicate network firing patterns. Dashed line represents minimum five spikes/100 ms.

(I) Spontaneous bursting in cultured cortical neurons. Synchronous bursting (defined as at least 25% of electrodes firing simultaneously) occurs (pink arrows); 16 electrodes per well. A mean of 12.2 electrodes (SD 1.87) contributed to network bursts of mean duration 13.3 ms.

(J) Hippocampal neurons exhibit greater spontaneous activity than cortical cultures over 10 min. A mean of 12.5 electrodes (SD 2.26) participated in network bursts with average duration 15.3 ms among hippocampal neurons.

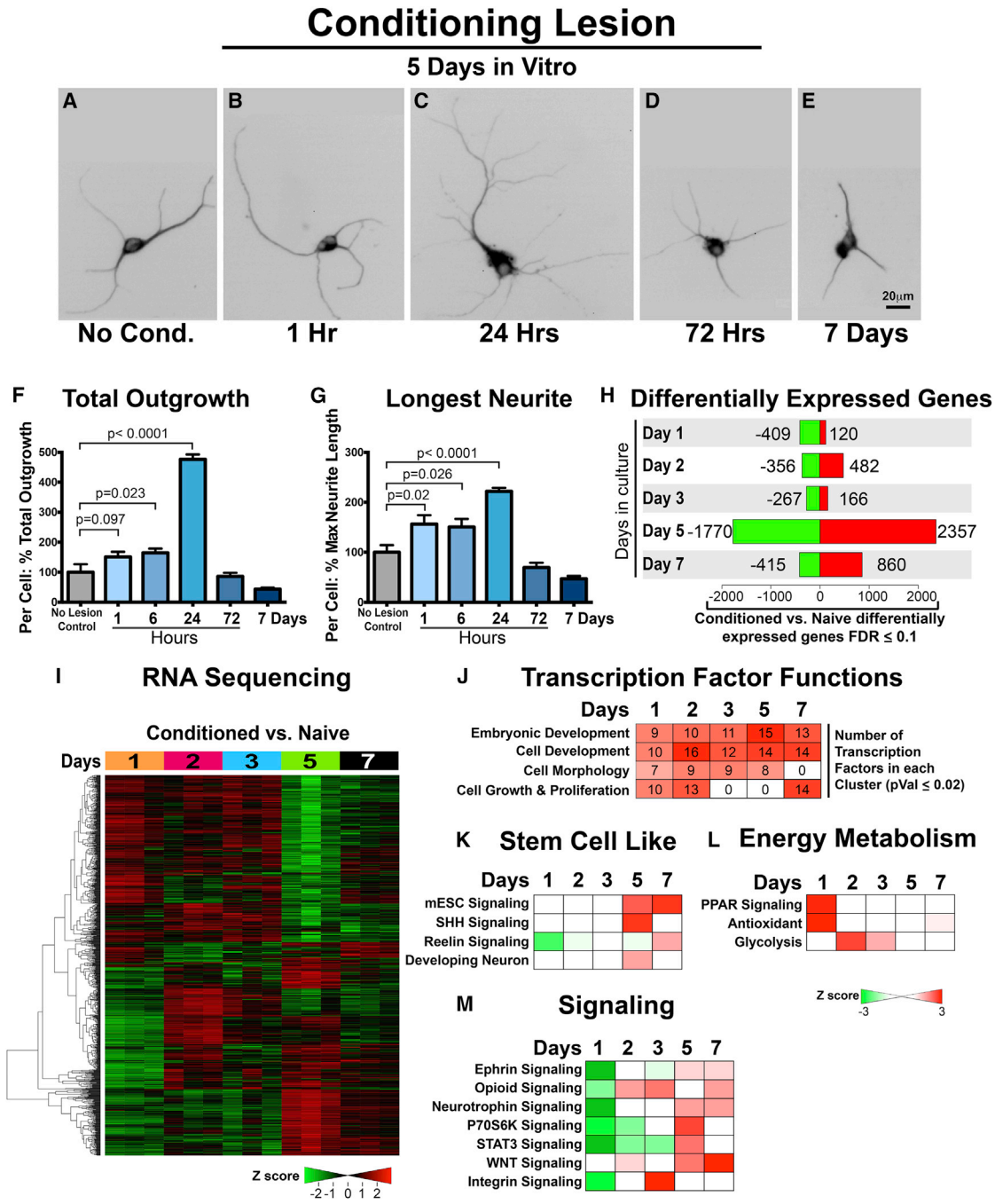

Figure 4. Conditioning lesions significantly enhance CNS cortical neurite growth

(A–E) The spinal cord was lesioned at C8; the motor cortex was then removed and cultured either (A) 1 h, (B) 6 h, (C) 24 h, (D) 72 h, or (E) 7 days later. All cells were then maintained for 5 days in culture. An increase in neurite length is particularly appreciable in cultures prepared 24 h after conditioning. Tuj1 label for neurons. Scale bar, 20 μm. Images of neurons were placed onto equal-sized background panels for presentation purposes.

(F and G) Total neurite length and (G) longest neurite length measured using Tuj1 labeling. N = 3 replicates, ± SEM There is a significant conditioning effect beginning 1 h after spinal cord injury and lasting 24 h.

(H) RNA sequencing of conditioned neuronal cultures. Spinal cord lesions were made 24 h before plating cells, and RNA sequencing was performed after 1, 2, 3, 5, and 7 days in culture. Number of differentially expressed genes (DEGs) compared with non-conditioned cultures sampled at the same number of days in culture are shown. FDR $\leq$0.1.

(I) Heatmap of top 1,000 differentially expressed genes (FDR $\leq$0.1, Benjamini-Hochberg adjusted p values) of conditioned relative to non-conditioned neurons at 1, 2, 3, 5, and 7 days in culture, arranged by hierarchical clustering. Red, increased expression; green, reduced expression. Intensity of color reflects degree of gene differential expression compared to non-conditioned cultures.

(legend continued on next page)

(Figures 2A and 3D). After 5 days *in vitro*, cortical motor neurons exhibited polarized morphology and expressed MAP2 in their dendritic and somatic compartments (Figure 2B), the specific axonal marker Tau in their axonal compartment (Figure 2C), and Tuj1 throughout all cellular processes. Thus, cultured neurons of the adult brain regained the characteristic features of their normal adult morphological and molecular state.

Time course of adult neuronal cultures

Using adult primary neurons from the motor cortex harvested at PND 38, we examined adult neuronal cultures serially over several days. Twenty-four hours after plating, individual round cells in culture had initiated outgrowth of single neurites up to 100 μm in length (Figures 3A and 3B). These initial processes did not exhibit identifiable growth cones. By 2 days in culture, additional neuritic processes emerged that were relatively uniform in caliber but continued to lack identifiable growth cones. However, by 3 days, cells began to exhibit asymmetric morphology, multiple neuritic extensions (Figure 3A), and a long major process (Figure 3A). Indeed, the leading edges of neuritic extensions contained lamellipodial structures typical of developing axons (Figure 3A, inset) (Bradke and Dotti, 1999). By 5 days *in vitro*, cells exhibited identifiable axonal processes (Figures 2B and 2C). The tips of many of these processes exhibited growth cones that appeared filamentous in nature (Figure 3C), again resembling structures observed in the developing nervous system (Figures 2D and 3A, inset). The axon-specific marker Tau was present in a single axonal extension from individual neurons, whereas the neuronal marker Tuj1 filled both axonal and dendritic processes (Figures 2B and 2C). Sholl analysis demonstrated steady increases in neuritic branching and complexity over successive days in culture (Figure 3B). Over serial days of growth, neuritic extension resulted in cell-to-cell contact and formation of synapses beginning at day 3, characterized by co-localization of Tuj1 and synaptophysin in sites of axonal/somal contact (Figure 2F). The post-synaptic scaffolding protein Homer was also present in these regions of axo-somatic apposition (Figure 2G), establishing conditions for synaptic activity.

Cultured adult neurons exhibit spontaneous and evoked electrophysiological activity

To determine whether adult neuronal cultures are synaptically active, we measured spontaneous and evoked electrical activity using a multi-electrode recording grid onto which cells were plated (Maestro, Axion Biosystems) (Marchetto et al., 2019). Starting with cultures of adult motor cortex and adult hippocampus isolated at postnatal day 42, we assessed spontaneous activity after 10 days in culture (Figure 3F). Both cortical and hippocampal adult neuronal cultures exhibited spontaneous bursts of activity (Figures 3F, 3I, and 3J). There was extensive synaptic inter-connectivity among motor cortex neurons *in vitro*: at least 76% of neurons exhibited synchronous firing patterns (Figure 3I) with a mean duration of 13.3 ms ± 2.8 (±SD). Adult hippocampal neurons also exhibited spontaneous activity and a similar degree of inter-connectivity (Figure 3J). To assess evoked activity, we depolarized a single electrode at 500 mV for 0.4 s every 5 s and recorded from the remaining 15 electrodes. Responses were observed every time a stimulus was applied (Figures 3G and 3H). Thus, cultures of primary adult neurons from both the motor cortex and hippocampus were synaptically active and exhibited activity in correlated networks.

Importance of adult neuronal cultures: Identification of a "conditioning" effect in adult motor cortex after spinal cord injury

The ability to culture neurons of the adult brain has the potential to contribute to a greater understanding of fundamental neural physiology and disease. To demonstrate this potential, we explored whether adult cortical neurons exhibited a "conditioning" response. One of the most mechanistically informative observations in decades in understanding axonal regeneration has been the phenomenon of the peripheral nerve "conditioning lesion": lesions of the *peripheral* process of DRG neurons "condition" the cell to regenerate both its central and peripheral processes more effectively (Ylera et al., 2009; Stam et al., 2007; De Virgiliis et al., 2020; Palmisano et al., 2019; Blesch et al., 2012; Mcquarrie et al., 1977; Mcquarrie and Grafstein, 1982). However, lesions of the *central* process of the DRG neuron do not increase growth of either the central or peripheral axonal branches. Identification of the molecular mechanisms associated with the peripheral conditioning effect used cultures of adult dorsal root ganglion neurons (Lankford et al., 1998; Seijffers et al., 2007) and led to candidate therapies that are undergoing clinical testing (Joy et al., 2019; Huebner et al., 2019). The inability to culture adult CNS neurons has deprived the field of an important tool in seeking corresponding discoveries relevant to regeneration of the brain and spinal cord (Poplawski et al., 2020; Chandran et al., 2016; Blesch et al., 2012; Renthal et al., 2020).

The present methods present a potential solution to this problem. To examine whether a "conditioning lesion" effect is present in the adult motor cortex after spinal cord injury, 15 adult C57BL/6J mice (age 42 days) were subjected to cervical spinal cord lesions that transected the corticospinal projection. We then euthanized animals 1, 6, 24, or 72 h and 7 days after the injury (n = 3 per time point) and prepared cultures of the adult motor cortex (Figures 4A–4E). The total extent of neurite outgrowth

(J) Pathway analysis of differentially expressed genes over days 1 to 7 in culture. The most significant clusters of transcription factor genes were related to embryonic development, cell morphology, and cell growth and proliferation, suggesting conversion of the cell to an immature growth state. State of activity of signaling pathway is represented by *Z* score (right-tailed Fisher exact test). Red, activation; green, inhibition. Scaling parameters listed at bottom right. n = 3 biological replicates for each day and condition.

(K) Pathway analysis supports the emergence of a stem cell-like transcriptional state after 5–7 days in culture.

(L) On the very earliest days of culture, cells exhibit marked elevations in cell metabolic, anti-oxidant and glycolytic pathways, indicating an abrupt transition to a state that may foster cell survival after removal from the brain. This state rapidly diminishes.

(M), General signaling pathways show early reductions in many trophic and guidance pathways, followed by their recovery starting approximately 3 days after culture as cells extend neurites and form synapses.

was assessed 5 days later, a time point used in many peripheral nerve conditioning studies.

We found a highly significant and substantial central conditioning effect: animals that received a spinal cord injury 24 h before preparation of motor cortex cultures exhibited a 4-fold increase in total neurite outgrowth compared with cortical neurons from controls that did not have a preceding spinal cord lesion (overall ANOVA $p < 0.0001$; post hoc Fischer's comparing intact to 24 h, $p < 0.0001$; Figure 4F). Cultures also demonstrated a 2-fold increase in longest neurite length ($p < 0.0001$) (Figure 4G). The conditioning effect peaked 24 h after injury; time points of 1 and 6 h post-injury also exhibited a significant conditioning effect of 1.5- and 1.6-fold, respectively, compared with non-preconditioned cultures ($p < 0.09$ and $p < 0.02$, respectively; Figures 4F and 4G). Notably, time points of 72 h and 7 days no longer supported a conditioning effect (Figures 4F and 4G), in contrast to findings in conditioned DRG neurons, which sustained a conditioning effect up to 1 week post-injury (Smith and Skene, 1997; Lankford et al., 1998; Renthal et al., 2020).

To identify the molecular mechanisms associated with the conditioning effect in cortical neurons, we performed RNA sequencing using the Illumina format (Poplawski et al., 2020). Mice at age 42 days (N = 15) underwent cervical spinal cord lesions to transect the corticospinal projection. Twenty-four hours after conditioning lesions (the time point that had the greatest effect on neurite outgrowth, Figures 4A–4G), we established cultures of the motor cortex (Figure S2B). We then isolated RNA from these cultures 24, 48, 72 h, 5 days, and 7 days after plating cells, and we compared findings with non-conditioned motor cortex cultures sampled at these same time points. Each time point had three replicates per group (conditioned and non-conditioned). We chose to sample 1, 2, 3, 5, and 7 days after culture for RNA sequencing because these time periods represented a range of early to late time points that we hypothesized included early transcriptional regulators of the regeneration response, a middle period that reflected active neurite extension and early synapse formation, and a late period of neuronal stabilization.

Cultures from conditioning lesions resulted in significant changes in gene expression compared with control cultures (Figures 4H–4 M). Using a false discovery rate (FDR) of $p \leq 0.1$, several hundred to several thousand genes were significantly differentially expressed at each time point compared with non-conditioned cultures (Figure 4H).

After 24 h in culture, conditioning lesions resulted in the significant upregulation of more than 100 genes. Among the most upregulated of these was the histone modifier "histone cluster 1, H3g" (*Hist1h3g*), exhibiting an 11-fold increase in expression in conditioned cultures versus non-conditioned cultures ($p = 6 \times 10^{-3}$). The DNA methyltransferase *Dnmt1* also increased 1.6-fold ($p = 1 \times 10^{-3}$) and the chromodomain helicase DNA-binding protein 1-like (Chd1l) exhibited a trend toward increase (4.5-fold, $p = 0.08$). The transcription factor *Gtf3c1* (general transcription factor III C 1) increased 3.2-fold ($p = 1 \times 10^{-4}$). Notably, in contrast to observations after peripheral nerve conditioning lesions, the transcription *ATF3* (activating transcription factor 3) was *downregulated* 4.2-fold ($p = 1 \times 10^{-4}$), whereas it is typically upregulated 12- to 16-fold at comparable time points after peripheral nerve conditioning lesions (Chandran et al., 2016; Seijffers et al., 2007). A large number of cell adhesion molecule genes were also upregulated, including cadherin 6 (*Cdh6*, increased 2.6-fold, $p = 3 \times 10^{-3}$) and protocadherins beta 5 (*Pcdhb5*, increased 4-fold, $p = 0.008$), alpha 9 (*Pcdha2*, increased 3.6-fold, $p = 0.02$), and gamma (*Pcdhga11*, increased 4-fold, $p = 4 \times 10^{-3}$). Doublecortin was also upregulated (*Dcx*, increased 2-fold, $p = 2 \times 10^{-4}$). In addition, the nerve growth factor receptor gene expression (*Ngfr*) increased 2-fold ($p = 0.05$). Overall, these changes in gene expression may be related to the accessibility of chromatin to undergo shifts that favor growth programs, the activation of transcription factors to support growth, and the expression of cell adhesion molecules that will favor physical extension of cellular processes.

Conditioning lesions also resulted in the significant *suppression* of more than 400 genes after 24 h in culture. Among these were pro-inflammatory genes, including interleukin 1 beta (downregulated 14-fold, $p = 1 \times 10^{-4}$), interferon-related genes (e.g., interferon activated gene 205 or *Ifi205*, downregulated 16-fold, $p = 1 \times 10^{-4}$), and chemokine genes (e.g., chemokine (C-X-C motif) ligand 3 or *Cxcl2*, downregulated 15-fold, $p = 1 \times 10^{-6}$) (Figure S3). Caspase 1 was also inhibited (downregulated 7.5-fold, $p = 1 \times 10^{-3}$). Structural cellular components were downregulated compared with non-conditioned cultures, including kinesin family members (kinesin *Kif12*, downregulated 9-fold, $p = 0.018$), dynein (*Dnah9* downregulated 5.6-fold, $p = 0.015$), actin (*actbl2* downregulated 5.4-fold, $p = 0.08$), and tubulin (*Tuba4a* downregulated 3.6-fold, $p = 1 \times 10^{-3}$). These changes suggest that conditioning lesions alter immune activation state, counter cell death pathways, and shift the dynamics of production of cytoskeletal components and transport.

Twenty-four hour culture data were further analyzed through the use of Ingenuity Pathway Analysis (IPA; QIAGEN, https://www.qiagenbioinformatics.com/products/ingenuitypathway-analysis) to identify primary transcriptional pathways and signaling hubs. This analysis revealed that conditioning lesions reduced the activation of signaling pathways reflecting reactive oxygen species, neuroinflammation, interleukin-8, and TREM1, and activated peroxisome proliferator activated receptor signaling (Figure S3). These patterns would generally appear to reduce the injury signal generated by the establishment of cell cultures.

After 48 h in culture, conditioning lesions resulted in the significant upregulation of nearly 500 genes (Figure 4H). Among these were the microRNA *Mir8115* (increased 17-fold, $p = 3 \times 10^{-3}$), integrin beta 1 binding protein (*Itgb1bp2*, increased 14-fold, $p = 2 \times 10^{-3}$), asparaginase homolog (*Aspg*, increased 10-fold, $p = 0.02$), hyaluronin and proteoglycan link protein 1 (*Hapln1*, increased 6-fold, $p = 4 \times 10^{-3}$), Rho GTPase-activating protein 20 (increased 2.7-fold, $p = 4 \times 10^{-4}$), and insulin-like growth factor 1 (*Igf1*, increased 2.3-fold, $p = 3 \times 10^{-6}$). Overall, these changes indicate an evolution toward more active gene expression of cellular signaling systems related to the growth state of cells (Zhang et al., 2019; Tan et al., 2015). Nearly 400 genes were also significantly downregulated (Figure 4H). Among these were histone cluster 4 (*Hist4h4*, reduced by 11-fold, $p = 7 \times 10^{-3}$), BRCA1 interacting protein C (*Brip1*, reduced by 16-fold, $p = 2 \times 10^{-4}$), forkhead box j1 (*Foxj1*, reduced 32-fold, $p = 6 \times 10^{-4}$), wingless-related MMTV

integration site 7B (*Wint7b*, reduced by 32-fold, $p = 4 \times 10^{-4}$), integrin beta 8 (*Itgb8*, reduced 12-fold, $p = 9 \times 10^{-4}$), ephrin receptors A4 and B4 (*Epha4* and *Ephb4*, both reduced 9.8-fold, $p = 1 \times 10^{-3}$ and 2×10^{-4} respectively), and semaphorins 3 and 5a (*Sema3g*, reduced 9-fold, $p = 1 \times 10^{-3}$; *sema* 5a, reduced 8-fold, $p = 6 \times 10^{-6}$). Differential expression of histones could lead to epigenetic changes representing a fundamental shift in accessibility of transcription factors; among these changes was the reduction of *Brip1*, *Foxj1,* and *Wnt* signaling that could activate the growth state of the cell. Changes in integrin receptors and guidance molecules would also influence neurite outgrowth (Tan et al., 2015; Eva and Fawcett, 2014). Ingenuity pathway analysis at 48 h in culture showed that conditioning lesions resulted in strong activation of oxidative phosphorylation and mitochondrial signaling and suppression of sirtuin signaling, compared with non-conditioned cultures, potentially playing a role in preparing the conditioned neurons to extend their neuritic network (Figure 4A). In addition, an enhancement in synaptogenic signaling was evident at this time period.

After 72 h in culture, there was a significant upregulation of approximately 150 genes. Histone deacetylase 9 (*Hdac9*) was upregulated 2-fold ($p = 0.01$). Once again, cell adhesion molecules remained upregulated as a function of the conditioning lesion, including integrin beta 1 binding protein (*Itgb1bp2*, increased 12-fold, $p = 4 \times 10^{-3}$), hyaluronin and proteoglycan link protein 1 (*Hapln1*, increased 7-fold, $p = 3 \times 10^{-3}$), and protocadherin gamma subunit (*Pcdhga11*, increased 3.7-fold, $p = 1 \times 10^{-4}$). Rho GTPase-activating protein 21 (*Arhgap21*) was increased 2-fold, and the tumor suppressor gene *Tusc3*, which is associated with cell "stemness," was upregulated 1.9-fold ($p = 4 \times 10^{-4}$). Ingenuity pathway analysis after 72 h in culture indicated that conditioning lesions now strongly favored signaling that supported synaptogenesis, glutamate receptors, synaptic long-term potentiation, and calcium signaling (Figure S4).

Five days in culture corresponded with a marked increase in the length of neurite growth in conditioned neurons compared with non-conditioned (Figure 4A), and at this time point there was a marked increase in differentially expressed genes: more than 4,000 genes reached significance when comparing conditioned with non-conditioned cultures (Figure 4H). Many of these were growth factor genes, including FGF2 (*Fgf2*, up 45-fold, $p = 1 \times 10^{-5}$), FGF16 (*Fgf16*, up 28-fold, $p = 3 \times 10^{-3}$), FGF7 (*Fgf7*, up 21-fold, $p = 1 \times 10^{-6}$), FGF4 (up 9-fold, $p = 0.02$), nerve growth factor (*Ngf*, up 8-fold, $p = 4 \times 10^{-5}$), BDNF (*Bdnf* up 17-fold, $p = 9 \times 10^{-4}$), IGF2 (up 16-fold, $p = 2 \times 10^{-4}$ and $p = 4 \times 10^{-4}$), and several IGF-binding proteins (e.g., *Igfbp6*; up 23-fold, $p = 4 \times 10^{-9}$). Beta tubulin, the microtubular protein gene, increased 12-fold ($p = 0.009$). A number of guidance and cell adhesion genes were also increased, including netrin 1 (*Ntn1*, up 8.5-fold, $p = 0.01$) and integrin alpha (*Itga2*, up 11-fold, $p = 6 \times 10^{-3}$). Among repressed genes were histone cluster H3a (*Hist1h3a*, down 15-fold, $p = 9 \times 10^{-3}$) and histone cluster 2, H2bb (*Hist2h2bb*, down 9-fold, $p = 2 \times 10^{-3}$), suggesting potential modifications to the chromatin that occurred as the cell modified its growth state and shifted toward stabilizing the cellular state. Ingenuity pathway analysis at 5 days in culture demonstrated the presence of Huntington's disease signaling as a hub (Poplawski et al., 2020), with reductions in synaptogenesis and protein kinase A signaling compared with non-conditioned cultures.

At the last time point studied in culture, 7 days, there were a total of approximately 1,200 differentially expressed genes comparing conditioned and non-conditioned cultures (Figure 4H). Among the upregulated genes were Notch2, which influences cell fate decisions (up 6-fold, $p = 1 \times 10^{-3}$) and the growth factor genes *FGF2* (up 40-fold, $p = 4 \times 10^{-5}$), and *Bdnf* (up 4-fold, $p = 0.03$). *Creb5*, related to the active state of the cell, was increased 11-fold ($p = 4 \times 10^{-3}$). Dynein axonemal assembly factor 3 (*Dnaaf3*) increased 100-fold compared with non-conditioned cultures ($p = 2 \times 10^{-5}$), suggesting more activity in establishing microtubular function. Cell adhesion and guidance molecules were also very actively upregulated, including protocadherin beat 21 (*Pcdhb21*, up 108-fold, $p = 4 \times 10^{-5}$), semaphorin 3a and 5a (*Sema3a*, up 32-fold, $p = 0.02$; *Sema5a*, up 13-fold, $p = 2 \times 10^{-4}$), *Wnt7b* (up 18-fold, $p = 1 \times 10^{-3}$), Ephrin receptors b1 and A4 (*Ephb1*, up 17-fold, $p = 1 \times 10^{-3}$; *Epha4* up 13-fold, $p = 2 \times 10^{-2}$), hyaluronan synthase (*Has2*, up 10-fold, $p = 1 \times 10^{-3}$), and hyaluronan and proteoglycan link protein 2 (*Hapln2*, up 15-fold, $p = 0.01$). Among downregulated genes were histone cluster 1 H4a (*Hist1h4a*, down 21-fold, $p = 1 \times 10^{-3}$) and histone cluster 2 H2bb (Hist2n2bb, down 5-fold, $p = 0.03$). Ingenuity pathway analysis demonstrated substantial activations of kinetochore metaphase signaling and suppression of *PTEN*, *BRCA1,* and cell cycline DNA damage checkpoint regulation, potentially reflecting ongoing cell activity and establishment of cellular networks in the dish, compared with non-conditioned cultures. Overall, later culture time points also exhibited the emergence of stem cell-like canonical pathways (Figures 4J, 4K, and S5).

DISCUSSION

The ability to culture mature, adult CNS neurons offers unprecedented opportunities for mechanistic discovery research and therapeutic development. These cultures faithfully reflect the intact morphological and neurotransmitter phenotype of their regions of sampling while exhibiting diversity between different isolation sites in cell size, morphology, and neurite outgrowth. Emerging axons elaborate growth cones that replicate neural development (Santos et al., 2020; Dotti et al., 1988), and cultures are synaptically active and rapidly form correlated networks *in vitro*, allowing electrophysiological study. Cultures are highly enriched for neurons (83% of cultured cells), and the residual presence of glia is likely useful in supporting neuronal survival, function, and extension of neuritic processes, as previously documented in embryonic and early postnatal neuronal cultures (Ullian et al., 2001; Paşca et al., 2015). As cultures develop, axon guidance molecules are expressed, including netrins and semaphorins, together with synaptic proteins including NMDA and AMPA receptors.

Highlighting the utility of this model system, we demonstrated the presence of a "conditioning lesion" effect in the CNS: following spinal cord injury, adult cortical neuron cultures express a highly significant, 4-fold increase in neurite outgrowth. This central neuronal conditioning effect is faster (peaking at

24 h) and greater in magnitude that a peripheral DRG neuron conditioning effect; the latter typically increases neurite growth 2.5-fold and is detectable from 2 to 7 days in culture (Smith and Skene, 1997). Because peripheral axons regenerate and central axons do not, we hypothesized that CNS neurons would lack a conditioning effect, but surprisingly we found the opposite. Moreover, previously it has been reported that lesions of the *peripheral* process of the DRG neuron result in a conditioning effect, whereas lesions of the *central* process (a spinal cord lesion) do not (Blesch et al., 2012). Yet now we find that a lesion of the central process of the CNS neuron successfully elicits a conditioning effect. Thus, injured PNS and CNS neurons respond differently to injury in several respects. Among these differences is the identity of transcription factors recruited by conditioning: the predominant transcription factor activated by a peripheral conditioning lesion is ATF-3, whereas this gene is actually suppressed in adult motor neuron cultures after conditioning. These findings highlight the importance of the ability to culture adult CNS neurons to detect these fundamental differences: pro-regenerative approaches to enhance PNS regeneration may not impact injured central neurons, a hypothesis supported by some experimental findings to date (Chandran et al., 2016; Sachdeva et al., 2016; Hiltonand Bradke, 2017). Separate tools are therefore needed to identify pro-regenerative approaches in the CNS. The CNS conditioning effect harnesses developmental programs, consistent with our previous *in vivo* observations (Poplawski et al., 2020).

There have been previous efforts to culture adult mammalian CNS neurons, resulting in very modest success (Carbonetto et al., 1987). Many of these attempts used FGF2 (Brewer, 1997; Brewer and Torricelli, 2007) in the culture medium, a growth factor that enhances the survival of immature neural progenitors and keeps them in an immature state (Palmer et al., 1995; Gage et al., 1995); accordingly, cells isolated using FGF2 might have been neural progenitor cells rather than mature neurons. In contrast, the method described here isolates adult neurons independent of FGF2 support, using BDNF, which supports neuronal differentiation and mature neuronal survival (Ahmed et al., 1995; Alderson et al., 1990; Giehl and Tetzlaff, 1996; Nagahara et al., 2009). Neural progenitor cells from the adult brain can be cultured from the hippocampal dentate gyrus and subventricular zone, but terminally differentiated, fully mature neurons have proven to be extraordinarily difficult to culture (Palmer et al., 1995; Gage et al., 1995; Brewer and Torricelli, 2007). This difficulty is likely because the process of removing adult neurons involves shearing the majority of their projections and cytoplasm, generating a terminal event for cells. The method described here gently and gradually dissociates cells, likely enabling adaptation that eventually generates more than 10,000 neurons per brain region, and consistently viable cultures. This number is sufficient to serve medium throughput screening for drug development, disease modeling, and regeneration, where neurons isolated from one animal can be plated at medium density within a 96-well culture vessel (Lowell et al., 2021; Al-Ali et al., 2017; Song et al., 2002). This number of cultured neurons also constitutes the plating density used in previous studies of embryonic and postnatal hippocampal cultures (Song et al., 2002; Al-Ali et al., 2017).

Study limitations

While achieving successful cultures of 10,000 *adult* neurons per brain region is a substantial advance that can be used in hypothesis-driven experimentation and low-to-medium output drug screening, high-throughput drug screens require much larger numbers of neurons that can be established as cell lines. The vast majority of neurons isolated by these methods are excitatory neurons, and assays that require or focus on greater proportions of inhibitory neurons will require further method development, likely using selective antibody screening to enrich for inhibitory cells. And the results published herein have only scratched the surface of this tool: for example, can one culture aged neurons, or neurons bearing human disease-causing mutations? It also remains to be determined whether these techniques will allow successful culture of human neurons. If so, access to adult neurons could markedly improve research into adult human brain neural mechanisms and disease. For example, a standard contemporary model for human CNS study is the induced pluripotent stem cell (IPSC)-derived human neuron. However, neurons that are described as ''mature'' in the IPSC literature are transcriptionally equivalent in many cases to developing or postnatal neurons rather than mature neurons (Studer et al., 2015; Mertens et al., 2018). While extremely valuable, the study of IPSC-derived neurons and neural progenitors in culture could yield distinct findings from adult and aged neurons. Directly induced neurons are superior to IPSCs in retaining the age characteristics of the starter cell (Mertens et al., 2018), but whether they reflect all features of the fully mature neuron is not entirely clear. The present findings provide the potential to actually study adult and aged neurons of both the normal and diseased brain.

Conclusion

We described methods for culturing adult CNS neurons that faithfully replicate many features of *in vivo* neurons of these brain regions. These methods offer a new and valuable tool for studying the mechanisms of normal brain neurons on many levels, and diseases of the brain.

STAR★METHODS

Detailed methods are provided in the online version of this paper and include the following:

- KEY RESOURCES TABLE
- RESOURCE AVAILABILITY
  - Lead contact
  - Materials availability
  - Data and code availability
- EXPERIMENTAL MODEL AND SUBJECT DETAILS
  - Tissue harvesting
  - Animal surgeries
- METHOD DETAILS
  - Tissue dissociation
  - Debris removal
  - Red blood cell removal
  - Neuronal enrichment
  - Magnetic separation

- Absolute neuron number
- Plating neurons in culture vessels
- Flow cytometry
- Microelectrode arrays
- Immunolabeling
- RNA sequencing
- Sholl analysis
- Neurite outgrowth

- QUANTIFICATION AND STATISTICAL ANALYSIS

SUPPLEMENTAL INFORMATION

Supplemental information can be found online at https://doi.org/10.1016/j.crmeth.2022.100255.

ACKNOWLEDGMENTS

This work was supported by the Dr. Miriam and Sheldon G. Adelson Medical Research Foundation, Wings for Life (WFL-US-12-17 8980EA), and the Veterans Administration (Gordon Mansfield Consortium for Spinal Cord Regeneration). Illustrations were painted by Elize Hagen Els (www.ElizeEls.com).

AUTHOR CONTRIBUTIONS

Conceptualization, E.V.N. and M.H.T.; methodology, E.V.N.; investigation, E.V.N., K.G., C.F.M., M.C.M, and R.K.; data analysis, E.V.N., R.K., and K.G.; supervision, S.D., F.B., D.H.G., F.H.G., and M.H.T.; resources, M.H.T, D.H.G, and F.H.G.; writing – original draft, E.V.N. and M.H.T.; writing – review & editing, E.V.N, S.D., F.B., F.H.G., and M.H.T.

DECLARATION OF INTERESTS

The authors declare no competing interests.

Received: February 11, 2022
Revised: May 10, 2022
Accepted: June 17, 2022
Published: July 18, 2022

REFERENCES

Ahmed, S., Reynolds, B.A., and Weiss, S. (1995). Bdnf enhances the differentiation but not the survival of cns stem cell-derived neuronal precursors. J. Neurosci. *15*, 5765–5778. https://doi.org/10.1523/jneurosci.15-08-05765.1995.

Al-Ali, H., Beckerman, S.R., Bixby, J.L., and Lemmon, V.P. (2017). In vitro models of axon regeneration. Exp. Neurol. *287*, 423–434. https://doi.org/10.1016/j.expneurol.2016.01.020.

Alderson, R.F., Alterman, A.L., Barde, Y.A., and Lindsay, R.M. (1990). Brain-derived neurotrophic factor increases survival and differentiated functions of rat septal cholinergic neurons in culture. Neuron *5*, 297–306. https://doi.org/10.1016/0896-6273(90)90166-d.

Blesch, A., Lu, P., Tsukada, S., Alto, L.T., Roet, K., Coppola, G., Geschwind, D., and Tuszynski, M.H. (2012). Conditioning lesions before or after spinal cord injury recruit broad genetic mechanisms that sustain axonal regeneration: superiority to camp-mediated effects. Exp. Neurol. *235*, 162–173. https://doi.org/10.1016/j.expneurol.2011.12.037.

Bradke, F., and Dotti, C.G. (1999). The role of local actin instability in axon formation. Science *283*, 1931–1934. https://doi.org/10.1126/science.283.5409.1931.

Brewer, G.J., and Torricelli, J.R. (2007). Isolation and culture of adult neurons and neurospheres. Nat. Protoc. *2*, 1490–1498. https://doi.org/10.1038/nprot.2007.207.

Brewer, G.J. (1997). Isolation and culture of adult rat hippocampal neurons. J. Neurosci. Methods *71*, 143–155. https://doi.org/10.1016/s0165-0270(96)00136-7.

Carbonetto, S., Evans, D., and Cochard, P. (1987). Nerve fiber growth in culture on tissue substrata from central and peripheral nervous systems. J. Neurosci. *7*, 610–620. https://doi.org/10.1523/jneurosci.07-02-00610.1987.

Carrel, A. (1923). A method for the physiological study of tissues in vitro. J. Exp. Med. *38*, 407–418. https://doi.org/10.1084/jem.38.4.407.

Chandran, V., Coppola, G., Nawabi, H., Omura, T., Versano, R., Huebner, E.A., Zhang, A., Costigan, M., Yekkirala, A., Barrett, L., et al. (2016). A systems-level analysis of the peripheral nerve intrinsic axonal growth program. Neuron *89*, 956–970. https://doi.org/10.1016/j.neuron.2016.01.034.

De Virgiliis, F., Hutson, T.H., Palmisano, I., Amachree, S., Miao, J., Zhou, L., Todorova, R., Thompson, R., Danzi, M.C., Lemmon, V.P., et al. (2020). Enriched conditioning expands the regenerative ability of sensory neurons after spinal cord injury via neuronal intrinsic redox signaling. Nat. Commun. *11*, 6425. https://doi.org/10.1038/s41467-020-20179-z.

Dotti, C.G., Sullivan, C.A., and Banker, G.A. (1988). The establishment of polarity by hippocampal neurons in culture. J. Neurosci. *8*, 1454–1468. https://doi.org/10.1523/jneurosci.08-04-01454.1988.

Eva, R., and Fawcett, J. (2014). Integrin signalling and traffic during axon growth and regeneration. Curr. Opin. Neurobiol. *27*, 179–185. https://doi.org/10.1016/j.conb.2014.03.018.

Gage, F.H., Coates, P.W., Palmer, T.D., Kuhn, H.G., Fisher, L.J., Suhonen, J.O., Peterson, D.A., Suhr, S.T., and Ray, J. (1995). Survival and differentiation of adult neuronal progenitor cells transplanted to the adult brain. Proc. Natl. Acad. Sci. USA *92*, 11879–11883. https://doi.org/10.1073/pnas.92.25.11879.

Giehl, K.M., and Tetzlaff, W. (1996). Bdnf and nt-3, but not ngf, prevent axotomy-induced death of rat corticospinal neurons in vivo. Eur. J. Neurosci. *8*, 1167–1175. https://doi.org/10.1111/j.1460-9568.1996.tb01284.x.

Harrison, R.G. (1910). The outgrowth of the nerve fiber as A mode of protoplasmic movement. J. Exp. Zool. https://doi.org/10.1002/jez.1400090405.

Hilton, B.J., and Bradke, F. (2017). Can injured adult cns axons regenerate by recapitulating development? Development *144*, 3417–3429. https://doi.org/10.1242/dev.148312.

Huebner, E.A., Budel, S., Jiang, Z., Omura, T., Ho, T.S.Y., Barrett, L., Merkel, J.S., Pereira, L.M., Andrews, N.A., Wang, X., et al. (2019). Diltiazem promotes regenerative axon growth. Mol. Neurobiol. *56*, 3948–3957. https://doi.org/10.1007/s12035-018-1349-5.

Joy, M.T., Ben Assayag, E., Shabashov-Stone, D., Liraz-Zaltsman, S., Mazzitelli, J., Arenas, M., Abduljawad, N., Kliper, E., Korczyn, A.D., Thareja, N.S., et al. (2019). Ccr5 is A therapeutic target for recovery after stroke and traumatic brain injury. Cell *176*, 1143–1157.e13. https://doi.org/10.1016/j.cell.2019.01.044.

Lankford, K.L., Waxman, S.G., and Kocsis, J.D. (1998). Mechanisms of enhancement of neurite regeneration in vitro following A conditioning sciatic nerve lesion. J. Comp. Neurol. *391*, 11–29. https://doi.org/10.1002/(sici)1096-9861(19980202)391:1<11::aid-cne2>3.0.co;2-u.

Levison, S.W., and Goldman, J.E. (1993). Both oligodendrocytes and astrocytes develop from progenitors in the subventricular zone of postnatal rat forebrain. Neuron *10*, 201–212. https://doi.org/10.1016/0896-6273(93)90311-e.

Lois, C., and Alvarez-Buylla, A. (1994). Long-distance neuronal migration in the adult mammalian brain. Science *264*, 1145–1148. https://doi.org/10.1126/science.8178174.

Lowell, J.A., O'neill, N., Danzi, M.C., Al-Ali, H., Bixby, J.L., and Lemmon, V.P. (2021). Phenotypic screening following transcriptomic deconvolution to identify transcription factors mediating axon growth induced by A kinase inhibitor. SLAS Discov. *26*, 1337–1354. https://doi.org/10.1177/24725552211026270.

Marchetto, M.C., Hrvoj-Mihic, B., Kerman, B.E., Yu, D.X., Vadodaria, K.C., Linker, S.B., Narvaiza, I., Santos, R., Denli, A.M., Mendes, A.P., et al. (2019). Species-specific maturation profiles of human, chimpanzee and bonobo neural cells. Elife *8*, e37527. https://doi.org/10.7554/elife.37527.

Mcquarrie, I.G., and Grafstein, B. (1982). Protein synthesis and axonal transport in goldfish retinal ganglion cells during regeneration accelerated by A conditioning lesion. Brain Res. *251*, 25–37. https://doi.org/10.1016/0006-8993(82)91270-7.

Mcquarrie, I.G., Grafstein, B., and Gershon, M.D. (1977). Axonal regeneration in the rat sciatic nerve: effect of A conditioning lesion and of dbcamp. Brain Res. *132*, 443–453. https://doi.org/10.1016/0006-8993(77)90193-7.

Mertens, J., Reid, D., Lau, S., Kim, Y., and Gage, F.H. (2018). Aging in A dish: ipsc-derived and directly induced neurons for studying brain aging and age-related neurodegenerative diseases. Annu. Rev. Genet. *52*, 271–293. https://doi.org/10.1146/annurev-genet-120417-031534.

Nagahara, A.H., Merrill, D.A., Coppola, G., Tsukada, S., Schroeder, B.E., Shaked, G.M., Wang, L., Blesch, A., Kim, A., Conner, J.M., et al. (2009). Neuroprotective effects of brain-derived neurotrophic factor in rodent and primate models of alzheimer's disease. Nat. Med. *15*, 331–337. https://doi.org/10.1038/nm.1912.

Palmer, T.D., Ray, J., and Gage, F.H. (1995). Fgf-2-Responsive neuronal progenitors reside in proliferative and quiescent regions of the adult rodent brain. Mol. Cell. Neurosci. *6*, 474–486. https://doi.org/10.1006/mcne.1995.1035.

Palmisano, I., Danzi, M.C., Hutson, T.H., Zhou, L., Mclachlan, E., Serger, E., Shkura, K., Srivastava, P.K., Hervera, A., Neill, N.O., et al. (2019). Epigenomic signatures underpin the axonal regenerative ability of dorsal root ganglia sensory neurons. Nat. Neurosci. *22*, 1913–1924. https://doi.org/10.1038/s41593-019-0490-4.

Paşca, A.M., Sloan, S.A., Clarke, L.E., Tian, Y., Makinson, C.D., Huber, N., Kim, C.H., Park, J.Y., O'rourke, N.A., Nguyen, K.D., et al. (2015). Functional cortical neurons and astrocytes from human pluripotent stem cells in 3d culture. Nat. Methods *12*, 671–678. https://doi.org/10.1038/nmeth.3415.

Poplawski, G.H.D., Kawaguchi, R., Van Niekerk, E., Lu, P., Mehta, N., Canete, P., Lie, R., Dragatsis, I., Meves, J.M., Zheng, B., et al. (2020). Injured adult neurons regress to an embryonic transcriptional growth state. Nature *581*, 77–82. https://doi.org/10.1038/s41586-020-2200-5.

Renthal, W., Tochitsky, I., Yang, L., Cheng, Y.C., Li, E., Kawaguchi, R., Geschwind, D.H., and Woolf, C.J. (2020). Transcriptional reprogramming of distinct peripheral sensory neuron subtypes after axonal injury. Neuron *108*, 128–144.e9. https://doi.org/10.1016/j.neuron.2020.07.026.

Reynolds, B.A., and Weiss, S. (1992). Generation of neurons and astrocytes from isolated cells of the adult mammalian central nervous system. Science *255*, 1707–1710. https://doi.org/10.1126/science.1553558.

Sachdeva, R., Theisen, C.C., Ninan, V., Twiss, J.L., and Houlé, J.D. (2016). Exercise dependent increase in axon regeneration into peripheral nerve grafts by propriospinal but not sensory neurons after spinal cord injury is associated with modulation of regeneration-associated genes. Exp. Neurol. *276*, 72–82. https://doi.org/10.1016/j.expneurol.2015.09.004.

Santos, T.E., Schaffran, B., Broguière, N., Meyn, L., Zenobi-Wong, M., and Bradke, F. (2020). Axon growth of cns neurons in three dimensions is amoeboid and independent of adhesions. Cell Rep. *32*, 107907. https://doi.org/10.1016/j.celrep.2020.107907.

Scott, B.S. (1977). Adult mouse dorsal root ganglia neurons in cell culture. J. Neurobiol. *8*, 417–427. https://doi.org/10.1002/neu.480080503.

Seijffers, R., Mills, C.D., and Woolf, C.J. (2007). Atf3 increases the intrinsic growth state of drg neurons to enhance peripheral nerve regeneration. J. Neurosci. *27*, 7911–7920. https://doi.org/10.1523/jneurosci.5313-06.2007.

Smith, D.S., and Pate Skene, J.H. (1997). A transcription-dependent switch controls competence of adult neurons for distinct modes of axon growth. J. Neurosci. *17*, 646–658. https://doi.org/10.1523/jneurosci.17-02-00646.1997.

Song, H.J., Stevens, C.F., and Gage, F.H. (2002). Neural stem cells from adult Hippocampus develop essential properties of functional cns neurons. Nat. Neurosci. *5*, 438–445. https://doi.org/10.1038/nn844.

Stam, F.J., Macgillavry, H.D., Armstrong, N.J., de Gunst, M.C.M., Zhang, Y., Van Kesteren, R.E., Smit, A.B., and Verhaagen, J. (2007). Identification of candidate transcriptional modulators involved in successful regeneration after nerve injury. Eur. J. Neurosci. *25*, 3629–3637. https://doi.org/10.1111/j.1460-9568.2007.05597.x.

Studer, L., Vera, E., and Cornacchia, D. (2015). Programming and reprogramming cellular age in the era of induced pluripotency. Cell Stem Cell *16*, 591–600. https://doi.org/10.1016/j.stem.2015.05.004.

Suhonen, J.O., Peterson, D.A., Ray, J., and Gage, F.H. (1996). Differentiation of adult hippocampus-derived progenitors into olfactory neurons in vivo. Nature *383*, 624–627. https://doi.org/10.1038/383624a0.

Tan, C.L., Kwok, J.C., Heller, J.P., Zhao, R., Eva, R., and Fawcett, J.W. (2015). Full length talin stimulates integrin activation and axon regeneration. Mol. Cell. Neurosci. *68*, 1–8. https://doi.org/10.1016/j.mcn.2015.03.011.

Ullian, E.M., Sapperstein, S.K., Christopherson, K.S., and Barres, B.A. (2001). Control of synapse number by glia. Science *291*, 657–661. https://doi.org/10.1126/science.291.5504.657.

Ylera, B., Ertürk, A., Hellal, F., Nadrigny, F., Hurtado, A., Tahirovic, S., Oudega, M., Kirchhoff, F., and Bradke, F. (2009). Chronically cns-injured adult sensory neurons gain regenerative competence upon A lesion of their peripheral axon. Curr. Biol. *19*, 930–936. https://doi.org/10.1016/j.cub.2009.04.017.

Zhang, Y., Williams, P.R., Jacobi, A., Wang, C., Goel, A., Hirano, A.A., Brecha, N.C., Kerschensteiner, D., and He, Z. (2019). Elevating growth factor responsiveness and axon regeneration by modulating presynaptic inputs. Neuron *103*, 39–51.e5. https://doi.org/10.1016/j.neuron.2019.04.033.

STAR★METHODS

KEY RESOURCES TABLE

REAGENT or RESOURCE	SOURCE	IDENTIFIER
Antibodies		
Biotin-Antibody Cocktail	Miltenyi	130-115-390
Anti-O4-PE	Miltenyi	130-095-887; RRID: AB_10831029
anti-CD45-VioBlue	Miltenyi	130-109-199
anti-CD11b-VioBright-FITC	Miltenyi	130-113-803; RRID: AB_2819369
anti-ACSA-2-allophycocyanin (APC)	Miltenyi	130-102-315; RRID: AB_2651190
Tuj1-APC antibody	Sony	4606095
CTIP2-488	Abcam	AB18465; RRID: AB_2064130
GAD1-APC	LSBio	C516965
VGlut1-APC	Miltenyi	130-120-765; RRID: AB_2857536
mouse IgG2a-APC isotype control	Miltenyi	130-113-831; RRID: AB_2733441
rat IgG2a-488 isotype control	Miltenyi	130-126-951
human IgG1-APC isotype control	Thermo Fisher	31154; RRID: AB_243591
Tuj1	Biolegend	802001 lot# B216295; RRID: AB_2564645
Tuj1	Biolegend	801202 lot#B249869; RRID: AB_10063408
VGlut1	Millipore	AB5905 lot# 2987423; RRID: AB_2301751
Synaptophysin	Synaptic Systems	101006 lot# 1-3; RRID: AB_2622239
MAP2	Encor Bio	CPCA-MAP2 lot#7225-2; RRID: AB_2138173
Tau	Chemicon	MAB3420 lot# LV1616764
FezF2	Millipore	ABN428 lot# 3113895
CTB	List Biologics	703 lot# 7032A10; RRID: AB_10013220
ChAT	Millipore	AB144P lot# 3429630; RRID: AB_2079751
Calbindin	Chemicon	AB1778 lot# 21071010
donkey anti rabbit 488	Invitrogen	A21206 lot# 2072687
donkey anti rabbit 594	Invitrogen	A21207 lot# 1744751
donkey anti rabbit 647	Invitrogen	A31573 lot# 1964354
donkey anti mouse 488	Invitrogen	A21202 lot# 2090565
donkey anti mouse 594	Invitrogen	A21203 lot# 1820027
donkey anti mouse 647	Invitrogen	A31571 lot# 2045337
donkey anti goat 488	Invitrogen	A11055 lot# 2059218
donkey anti goat 594	Invitrogen	A11058 lot# 1842799
donkey anti goat 647	Invitrogen	A21447 lot#2045332
donkey anti guinea pig 488	Jackson Immuno	706-545-148 lot#140967
donkey anti guinea pig 594	Jackson Immuno	705-585-147 lot# 142483
donkey anti guinea pig 647	Jackson Immuno	706-605-148 lot# 143565
donkey anti chicken 488	Jackson Immuno	703-545-155 lot#144438
donkey anti chicken 594	Jackson Immuno	703-585-155 lot# 131340
donkey anti chicken 647	Jackson Immuno	703-605-155 lot#143668
Chemicals, peptides, and recombinant proteins		
calcein AM	Thermo Fisher	C1430
propidium iodide	Invitrogen	P3566
paraformaldehyde	TCI	P0018 lot#QNMDA IE
1XPBS	Gibco	14190-144 lot#2290385
BDNF	Peprotech	450-02

(*Continued on next page*)

Continued

REAGENT or RESOURCE	SOURCE	IDENTIFIER
MACS neuro media	Miltenyi	130-093-570
10% BSA sterile stock solution	Miltenyi	130-91-376
B27	Gibco	17504044
100X Glutamax	Gibco	35050061
100X Pen/strep	Sigma	P4333-20ML
FBS	Gibco	26140
70-μM cell strainer	Falcon	352350
0.01% poly-L-lysine	Sigma	P4707-50ML
Laminin	Sigma	L2020
Double distilled H_2O	Invitrogen	10-977-023
Nunc Lab-Tek II 8-well chambered slide	Sigma	Z734853-96EA
Cytoview MEA 48-well black plates	Axion	M768-tMEA-48B-5
DPBS with Ca^{2+} and Mg^{2+}, glucose, pyruvate	Gibco	14287072
DPBS with Ca^{2+} and Mg^{2+}	Gibco	14040141
Countbright Absolute counting beads	Thermo Fisher	C36950, lot# 2162689
Isoflurane gas	Covetrus	029405
1% Cholera Toxin B	List Biological Labs	104
Triton X-100	Fisher Scientific	BP151-100 lot#158296
Fluormount G	Southern Biotech	0100-01 lot#J1419-X889
Flow cytometry fixation buffer	R&D systems	FC004
Flow cytometry permeabilization/wash buffer	R&D systems	FC005
Cover Glasses	fisher Scientific	125485P lot#18846
Critical commercial assays		
Adult brain dissociation kit	Miltenyi	130-107-677
Neuron isolation kit	Miltenyi	130-115-390
Nugen Ovation RNA Ultra Low V2	Nugen	0344NB
Deposited data		
GEO DataSets: GSE205486		
Other		
GentleMACS Octo Dissociator with Heaters	Miltenyi	130-096-427
MidiMACS separator	Miltenyi	130-042-302
C-tubes	Miltenyi	130-096-334
LS-columns	Miltenyi	130-042-401
Maestro MEA system and AxIS software	Axion	
Magnetic Separator	Miltenyi	130-042-302
MACS multistand	Miltenyi	130-042-303
FACS Aria II Cell Sorter	BD Biosciences	P69500111, 4 lazer system
Novocyte 3000 analyzer	Agilent	RMNNC3000
Glass Capillaries	World Precision Instruments	1B150F-4
Picospritzer II	Parker Hannifin	
Kopf wire knife	David Kopf Instruments	
MACSQuant analyzer 10	Miltenyi	
Software and algorithms		
NovoExpress software	Agilent	version 1.5.0
MACSQuantify software	Miltenyi	version 2.10.1647.17442
FACSDiva software	BD Biosciences	Version 6.1.3
AxIS software	Axion Biosystems	Version 3.5.1
Fiji plugin Sholl Analysis	ImageJ	Version 3.1
ImageJ plugin NeuronJ	ImageJ	Version 1.4.1

RESOURCE AVAILABILITY

Lead contact

Further information and requests for resources and reagents should be directed to and will be fulfilled by the lead author, Erna van Niekerk (errrna@gmail.com).

Materials availability

This study did not generate new unique reagents.

Data and code availability

- RNA sequencing data reported in this manuscript have been deposited online at GEO DataSets: (https://www.ncbi.nlm.nih.gov/geo/query/acc.cgi?acc=GSE205486). Deposited data contains both raw fastq files and differential expression analysis. Raw fastq files are provided for each time point, condition, and replicate. Differential expression analysis consists of each conditioned time point compared to its un-conditioned time point control.
- This paper does not report any original code.
- Any additional information required to reanalyze the data reported in this paper is available from the lead contact upon request.

EXPERIMENTAL MODEL AND SUBJECT DETAILS

All procedures involving mice were carried out in strict adherence to guidelines provided by the Guide for the Care and Use of Laboratory Animals, and requirements of the institutional animal welfare committee (VASDHS Animal Care and Use Program Office IACUC_A13_42).

Tissue harvesting

Brain tissue was individually harvested from specific CNS regions, including the cortex, hippocampus, brainstem, cerebellum, and spinal cord. All tissue was isolated from C57 BL/6 mice aged 6 weeks or older, male and female unless otherwise stated. Each step was performed on ice with pre-cooled buffers and solutions. Vortexing was never used.

Neural tissue was rapidly removed as a block from an entire brain region (e.g., motor cortex, hippocampus, etc.) of the animal and immediately placed in Dulbecco's PBS (DPBS) with calcium (0.9 mM), magnesium (0.49 mM), glucose (5.5 mM) and sodium pyruvate (0.32 mM) (Gibco, 14287072) with 20 mg/ml Pen/Strep to remove any bacterial contamination. Tissue was then rinsed in five subsequent steps by transferring tissue through five wells containing DPBS with calcium, magnesium, glucose and pyruvate on ice to remove residual antibiotics.

Animal surgeries

All procedures were carried out in strict adherence to guidelines provided by The Guide for the Care and Use of Laboratory Animals and requirements of the institutional animal welfare committee. Animal subjects were C57 BL/6 mice aged 6 weeks or older, male and female unless otherwise stated. All surgeries were performed under deep anesthesia using isoflurane gas (Covetrus, 029405). CTB labeling was performed by exposing spinal level C8 and inserting a pulled glass pipette (World Precision Instruments, 1B150F-4) 0.5 mm lateral to midline, 0.6 mm deep. Using a picospritzer II (Parker Hannifin), 1 ul of 1% Cholera Toxin B (List Biological Labs, 104) was injected at a slow rate, injecting both left and right spinal cord. Dorsal column lesions were performed at spinal level C7 using a Kopf wire knife (David Kopf Instruments), 0.6 mm lateral to midline, 0.4 mm deep, and lifted to transect the dorsal column with coincident compression with a 28-ga blunt tip to ensure lesion completeness. Conditioning Lesion: dorsal column lesions were performed at spinal level C7 as described above. Cortices were isolated for culture at 1 hr, 6 hr, 24 hr, 72 h, and 7 days post lesion. Three animals were used per timepoint as individual biological replicates where each animal's cortical neurons were isolated, cultured, plated, and imaged individually.

METHOD DETAILS

This protocol is optimized for mouse tissue and was modified from Miltenyi adult brain dissociation (130-107-677) and adult neuron isolation (130-126-603) protocols.

Tissue dissociation

Tissue was weighed and transferred to gentleMACS C-tubes (Miltenyi, 130-096-334) containing enzyme mix 1 with papain at a final concentration of 250 μg/mL prepared from the Miltenyi adult brain dissociation kit (130-107-677). Once dissected, tissues were placed into C-tubes, and enzyme mix 2 containing DNAseI was added into the tube with tissue at a final concentration of 37 μg/ml. Tissue weight ranged from 20-500 mg per C-tube but was never allowed to exceed 500 mg. Sealed C-tubes were then transferred to the gentleMACS Octo Dissociator with heaters (Miltenyi, 130-096-427). The tube was secured in the instrument and

the heater cuff was placed over the tube to maintain 37°C throughout dissociation. This machine performed gentle dissociation of the tissue over a 30 min period, gradually gyrating the brain sample in the gentle enzyme mix.

Once dissocation was complete, C-tubes were removed and briefly centrifuged at 15- seconds pulse, never exceeding 300 g. All material was gently collected from the bottom of the tube using a pipette tip. The cellular material was then passed through a 70-μm cell strainer (Falcon, 352350) by first applying 2 mL DPBS with Ca^{2+} and Mg^{2+} (Gibco, 14040141) onto the strainer membrane and then gently applying the cellular material from the C-tube through the strainer. Ten mL DPBS with Ca^{2+} and Mg^{2+} was used to rinse the C-tube once, and then the cell material was applied through the cell strainer. Cellular material that passed through the strainer was then centrifuged at 300 g for 10 min at 4°C. Supernatant was asperated off and the pellet was resuspended in diluted debris removal solution.

Debris removal

A density gradient was used to separate viable cells from cellular debris within the sample in a 15-mL conical tube (ThermoFisher 339650). First, 900 μL debris removal solution (Miltenyi, 130-107-677) was diluted with 3.1 mL of DPBS containing Ca^{2+} and Mg^{2+} (Gibco, 14040141) and was triturated to mix well. To the cellular pellet, 4 mL of diluted debris removal solution were added to bring the total volume to ~4.4 mL. This volume was added gradually: 1 mL of diluted debris removal solution was first added and gently mixed, then the remaining 3 mL was added and gently mixed for a final volume of 4.4 mL of solution + cells. The 15-mL conical tube was gently tilted to the horizontal plane, and an additional 4 mL volume of DPBS with Ca^{2+} and Mg^{2+} was slowly overlaid in an effort to avoid perturbing the interface between the two solution densities. The conical tube was then moved to the vertical position and was centrifuged at 4°C, 3,000 g for 10 min. Samples were carefully removed so as not to mix the two fluid phases. A 1-mL pipette was used to remove a white band within the two phases that consisted of cellular debris. The conical tube was then filled to the top with DPBS with Ca^{2+} and Mg^{2+} and inverted three times to mix well the fluid solution but not disturb the cellular pellet. This tube was then centrifuged at 4°C, 1,000 g for 10 min. Supernatant was discarded.

Red blood cell removal

This step ensured the removal of red blood cells through hemolysis and prevented their contamination in culture. Red blood cell solution (Miltenyi, 130-096-334) (10X) was diluted 10-fold with sterile double-distilled water (ddH_2O) to generate a 1X solution that was supplemented with 0.02 μg/mL BDNF (Peprotech, 450-02). For volumes required, see Miltenyi (130-096-334). The cell pellet was gently resuspended in 1X red blood cell solution + BDNF until homogeneous and then incubated at 4°C, 10 min. This step was performed in a refrigerator for optimal temperature control to ensure red blood cell lysis. DPBS with Ca^{2+} and Mg^{2+} + 0.5% BSA was immediately added to the cell mixture and centrifuged at 4°C, 300 g for 10 min. For volumes to use, see Miltenyi (130-096-334). Supernatant was discarded.

Neuronal enrichment

This step was designed for the depletion of non-neuronal cells. This protocol uses antibodies specific for mouse surface antigens. To the cell pellet collected after red blood cell removal, 80 μL DPBS with Ca^{2+} and Mg^{2+} + 0.5% BSA was added. This volume is appropriate for a total number between $5 \times 10^6 - 4 \times 10^7$ cells. Twenty μL of non-neuronal cell Biotin-Antibody Cocktail (Miltenyi, 130-126-603) was added to the cell mixture and gently mixed. The cell mixture was incubated at 2–8°C for 5 min in a refrigerator to maintain constant temperature. One mL of DPBS with Ca^{2+} and Mg^{2+} + 0.5% BSA was then added and centrifuged at 300 g for 10 min at 4°C. Supernatant was discarded. For magnetic labeling, 80 μL DPBS with Ca^{2+} and Mg^{2+} + 0.5% BSA was added to pellet and gently resuspended. Twenty μL anti-Biotin Micro-Beads (Miltenyi, 130-126-603) were added to the mixture and gently mixed. The cell mixture was incubated at 2–8°C for 10 min in a refrigerator.

Magnetic separation

Magnetically bound non-neuronal cells were depleted from the cell population using a magnetic separator, whereas unlabeled neuronal cells flowed through the column and were captured in the flow-through. LS-columns (Miltenyi, 130-042-401) were inserted into a magnetic separator (Miltenyi, 130-042-302) placed onto a MACS multistand (Miltenyi, 130-042-303). Securing the column first by pressing it back and upright into the magnet, the LS-column was rinsed with 2 mL culture media and flow-through was allowed to flow completely by gravity. Once flow stopped, a new collection tube (15 mL conical) was placed at the bottom of the LS-column. To the final cell mixture from magnetic labeling, 400 μL culture media was added for a final 500 μL volume per one LS-column. The 500-μL cell mixture was applied to the top of the LS-column by directly pipetting into the column. The mixture was allowed to drain by gravity flow. Once flow stopped, 1 mL of culture media was added and allowed to drain until flow stopped (prepared as indicated in the next paragraph). Another 1 mL of culture media was added to the LS-column and allowed to drain until flow stopped. Neurons were collected through the column as the flow-through with a final volume of 2.5 mL.

Cell culture media consisted of MACS neuro media (Miltenyi, 130-093-570) supplemented with 10 mg/mL Glutamax (Gibco, 35050061), 10 mg/mL Pen/strep (Sigma, P4333-20 ML), 10 mg/mL B27 (Gibco, 17504044), and 100 mg/mL FBS (Gibco, 26140). BDNF was added fresh to the culture media for a final concentration of 0.02 μg/mL (Peprotech, 450-02).

Absolute neuron number

To determine the exact number of neurons isolated per cortex from 8-week-old subjects, Flow cytometry (BD Biosciences FACS Aria II Cell Sorter serial #P69500111 sorted with 100-μm nozzle at 20 psi, 4 lazer system) was performed on cells after neuronal enrichment and magnetic separation and analyzed with BD FACSDiva software (Version 6.1.3). Countbright Absolute counting beads were used (Thermo Fisher C36950, lot# 2162689). Calculation of cell concentration was (A/B) * (C/D), where A = number of viable cell events, B = number of bead events, C = bead lot count (Lot#2162689 = 51,500 beads/50 μL) and D = volume of sample.

Plating neurons in culture vessels

Culture vessels were prepared 24 h in advance and were acclimated to 37°C before plating. Sterile culture vessels were pre-coated with 0.01% poly-L-lysine (Sigma, P4707-50 ML) for a minimum of 1 h at room temperature under sterile conditions. Poly-L-lysine was removed and allowed to air-dry in the tissue culture hood. The culture vessel was briefly rinsed with ddH_2O and air dried. Twenty μg/ml laminin (Sigma, L2020) diluted in DPBS with Ca^{2+} and Mg^{2+} was added overnight at 4°C. Before adding cells, laminin was removed and enough culture media was added to cover the surface of the culture vessel. The culture vessel was warmed to 37°C and media was removed before cells were plated.

Neurons suspended in culture media were added to the culture vessel with BDNF at a final concentration of 0.02 μg/mL. Neurons were plated at a density of 3-4x10^4 cells/cm^2. Higher plating densities can also be made if network formation is desired. Cells were maintained at 37°C with 5% CO_2 in the sterile incubator. Culture media was replaced every two days by removing half the volume and supplementing with equal volume fresh cell culture media. BDNF was added at 0.04 μg/mL for a final concentration of 0.02 μg/mL. Cells could be maintained for 14 days in culture but, for longer cultures, astrocytes (ScienceCell #1800) were supplemented into culture vessels at a plating density of 4 × 10^4 cells/cm^2.

Flow cytometry

Flow cytometry was used to detect the presence of non-neuronal cells in the enriched neuronal fraction. Following brain dissociation and neuronal isolation of cortical tissue isolated at PND60, samples were exposed to the following antibodies: Anti-O4-PE (Miltenyi, 130-095-887, human, mouse, rat clone: REA576); anti-CD45-VioBlue (Miltenyi, 130-109-199, mouse clone:REA737); anti-CD11b-VioBright-FITC (Miltenyi, 130-113-803, mouse clone: REA592); anti-ACSA-2-allophycocyanin (APC) (Miltenyi, 130-102-315, mouse clone: IH3-18A3); and CD11b-VioBright-FITC (Miltenyi, 130-109-368, mouse clone:REA592) according to manufacturer's protocol. The MACSQuant analyzer 10 was used for sample acquisition and the MACSQuantify software (version 2.10.1647.17442) was used to analyze all samples. Three separate animals were used where each run consisted of at least 30,000 events.

To determine the percent of neurons or neuronal populations in the enriched neuronal fraction, after tissue dissociation and neuron enrichment, cells were briefly centrifuged at 300xg for 10 min and resuspended in 500 μL flow cytometry fixation buffer (R&D systems, FC004) and incubated for 10 min at room temp. Cells were washed with PBS and centrifuged again as above. Pellet was resuspended in 200 μL flow cytometry permeabilization/wash buffer (R&D systems, FC005) and Tuj1-APC antibody (Sony, 4606095) was added at 1:50 dilution; CTIP2-488 antibody (Abcam, AB18465) was added at 1:50 dilution; GAD1-APC (LSBio, C516965) was added at 1:50 dilution; VGlut1-APC (Miltenyi, 130-120-765) was added at 1:50 dilution; mouse IgG2a-APC isotype control (Miltenyi, 130-113-831) was added at 1:50 dilution; rat IgG2a-488 isotype control (MIltenyi, 130-126-951) was added at 1:50 dilution; and human IgG1-APC isotype control (Thermo Fisher, 31154). The mixture was incubated overnight at 4°C and excess antibody was removed by washing cells once with 1 mL flow cytometry permeabilization buffer, centrifuged and cell pellet resuspended in 200 μL PBS for flow cytometric analysis. The MACSQuant analyzer 10 was used for sample acquisition and the MACSQuantify software (version 2.10.1647.17442) was used to analyze samples; or the Agilent Novocyte 3000 analyzer (RMNNC3000) was used for sample acquisition and the NovoExpress (version 1.5.0) was used to analyze samples. Three separate animals were used per antibody (N = 3), where each run consisted of at least 30,000 events.

Following brain dissociation and neuron isolation, FACS analysis was used to determine the number of viable and dead cells isolated per animal. Three animals were used per timepoint and maintained separately. Once dissociated and enriched for neuron isolation, samples were incubated with calcein AM (Thermo Fisher, C1430) 1:1000 to detect viable cell number, and propidium iodide (Invitrogen, P3566) 1:1000 to determine the number of dead cells 30 min before analysis. A FACS Aria2 sorter was used for sample acquisition and FACSDiva software version 6.1.3 was used to analyze all samples. Three separate animals were used, where each run consisted of at least 30,000 events.

Microelectrode arrays

Cytoview MEA 48-well black plates (Axion, M768-tMEA-48B-5) were pre-coated with poly-L-lysine and laminin as described in the culture vessel reagent preparation section. Cortices and hippocampi were isolated and dissociated, and neurons were enriched as described above from 6-week-old mice. Cells were plated at a density of 1.2 × 10^5 cells per well according to Axion cell culture protocol and maintained at 37°C with 5% CO_2. Recordings were performed in a Maestro MEA system and AxIS software (*Axion Biosystems*) using a bandwidth with a filter for 10 Hz to 2.5 kHz cutoff frequencies. Spike detection was performed using an adaptive threshold set to 5.5 times the standard deviation of the estimated noise on each electrode. Each plate rested for 10 min for acclimatization in the Maestro instrument and was then recorded for an additional 10 min to calculate spike rates. Multi-electrode data analysis was performed using the Axion Biosystems Neural Metrics Tool. An active electrode was considered once five spikes occurred

over the length of 1 min (five spikes/min). Bursts were identified in the data recorded from each individual electrode using an adaptive Poisson surprise algorithm. Network bursts were identified for each well using a non-adaptive algorithm requiring a minimum of 10 spikes with a maximum inter-spike interval of 100 ms.

Immunolabeling

Cells were fixed by adding 8% paraformaldehyde (TCI P0018 lot#QNMDA IE) for a final concentration of 4% paraformaldehyde per well, and left standing for 20 min at room temperature. Media + PFA was gently removed and 1XPBS (Gibco 14190-144 lot#2290385) was added to cell, and held at room temperature for 30 min. To avoid cells being washed away, aspiration of media was performed gently by pipette. PBS was removed and cells were permeabilized and blocked with 5% donkey serum, 0.25% triton X100 (Fisher Sci BP151-100 lot#158296) in PBS for 1 h at room temperature while remaining stationary. Supernatant was gently removed and primary antibodies incubated in 5% donkey serum in PBS overnight at 4°C, held in a stationary position. The next day, primary antibody was removed and cells were washed with 1XPBS for 30 min at room temperature while remaining stationary. Secondary antibodies were diluted in 5% donkey serum in PBS, added to cells and incubated for 1 h at room temperature. Cells were washed with 1XPBS for 30 min at room temperature while remaining stationary and were then mounted using Fluormount G (Southern Biotech 0100-01 lot#J1419-X889) and coverslipped (fisher Sci 125485P lot#18846).

The following primary antibodies were used: Tuj1 1:10,000 (Biolegend 802001 lot# B216295); Tuj1 1:1000 (Biolegend 801202 lot#B249869); VGlut1 1:2000 (Millipore AB5905 lot# 2987423); Synaptophysin 1:500 (Synaptic systems 101006 lot# 1-3); MAP2 1:5000 (Encor Bio CPCA-MAP2 lot#7225-2); Tau 1:1000 (Chemicon MAB3420 lot# LV1616764); FezF2 1:500 (Millipore ABN428 lot# 3113895); CTB 1:5000 (List Biologics 703 lot# 7032A10) ChAT 1:200 (Millipore AB5905 lot# 3429630); Calbindin 1:1000 (Chemicon AB1778 lot# 21071010).

The following secondary antibodies were used: donkey anti rabbit 488 (Invitrogen A21206 lot# 2072687), donkey anti rabbit 594 (Invitrogen A21207 lot# 1744751), donkey anti rabbit 647 (Invitrogen A31573 lot# 1964354), donkey anti mouse 488 (Invitrogen A21202 lot# 2090565), donkey anti mouse 594 (Invitrogen A21203 lot# 1820027), donkey anti mouse 647 (Invitrogen A31571 lot# 2045337) donkey anti goat 488 (Invitrogen A11055 lot# 2059218), donkey anti goat 594 (Invitrogen A11058 lot# 1842799), donkey anti goat 647 (Invitrogen A21447 lot#2045332), donkey anti guinea pig 488 (Jackson Immuno 706-545-148 lot#140967) donkey anti guinea pig 594 (Jackson Immuno 705-585-147 lot# 142483), donkey anti guinea pig 647 (Jackson Immuno 706-605-148 lot# 143565), donkey anti chicken 488 (Jackson Immuno 703-545-155 lot#144438), donkey anti chicken 594 (Jackson Immuno 703-585-155 lot# 131340), donkey anti chicken 647 (Jackson Immuno 703-605-155 lot#143668).

RNA sequencing

The RNA library was prepared using Nugen Ovation RNA Ultra Low Input + Kapa Hyper over 2 planes by HiSeq4000. Reads were aligned to the latest mouse_mm10 reference genome using the STAR spliced read aligner. Total counts of read-fragments aligned to known gene regions within the mouse mm10 refSeq reference annotation were used as the basis for quantification of gene expression. Fragment counts were derived using HTS-seq program using mm10 Ensembl transcripts as the model. Several QC analyses were conducted to assess the quality of data and identify outliers. The Illumina QC read qualities were high, particularly the lower quartile base qualities with a Sanger Phred score of 53; based on this quality metric we did not exclude any samples or reads. One sample, naive day 7 replicate #3, failed library prep, most likely due to low starting material. Differentially expressed genes were identified using a bioconductor package edgeR with adjusted p-values (FDR) of $\leq$0.1. Standard differential gene expression analysis was performed (refSeq model) where normalized counts were regressed out for SeqPC1-3, and genes with a minimum of five counts for at least six samples were used. Differential expression analysis was conducted with R-project and the Bioconductor package edgeR (v.3.14.0)54. Statistical significance of differential expression was determined at FDR < 10% (q < 0.1). RNA sequencing data were analyzed both through inspection of lists of significantly differentially expressed genes (Figure S2, complete gene list) and using Ingenuity Pathway Analysis software (Qiagen) utilizing the complete gene list. We performed comparisons of Day 1 conditioned to Day 1 non-conditioned samples; comparisons of Day 2 conditioned to Day 2 non-conditioned samples; and so forth.

Sholl analysis

2D black and white images containing a single neuron per image labeled for Tuj1 were analyzed using the Fiji plugin Sholl Analysis (https://imagej.net/Sholl_Analysis version 3.1). The center of the soma was set as startup ROI, sholl radius set to 10 μm, and step size set to generate concentric circles every 1-μm interval up to 500 μm. The numbers of intersections were plotted as a function of radial distance from the soma to measure neurite complexity over time. Fifty images were analyzed for every timepoint and cell type.

Neurite outgrowth

2D 8-bit images of neurons labeled for Tuj1 were analyzed using the ImageJ plugin NeuronJ (https://imagej.net/NeuronJ version 1.4.1). All neurites per cell were traced where the longest neurite per cell was measured, as well as total neurites per cell measured. Biological replicates consisted of individual animals being cultured and plated individually, and neurons traced from these individual animals, where at least 50 neurons were traced per animal.

QUANTIFICATION AND STATISTICAL ANALYSIS

All bar graphs are presented as the mean +s.e.m. For quantification, an unpaired, two-tailed Student's *t* test was used.

For RNA-seq analysis, an FDR of 10% (FDR $q < 0.1$) was applied. For RNA sequencing we applied ranked gene expression by log-transformed fold change to both datasets individually. Experimenters were blinded to group identity when conducting experiments and performing analyses.